Hindawi
Geofluids
Volume 2021, Article ID 6631152, 23 pages
https://doi.org/10.1155/2021/6631152

*Research Article*

# A New Density Model of Quartz Solubility in $H_2O$-$CO_2$-NaCl Ternary Systems up to High Temperatures and High Pressures

**Weiping Deng**,[1] **Qing Wei**,[1,2] **and Xuan Liu**[3]

[1]*National Institute of Natural Hazards, Beijing 100085, China*
[2]*State Key Laboratory of Ore Deposit Geochemistry, Institute of Geochemistry, Chinese Academy of Sciences, Guiyang 550081, China*
[3]*Université de Lorraine, CNRS, CREGU, GeoRessources, F-54000 Nancy, France*

Correspondence should be addressed to Qing Wei; qingwei@ninhm.ac.cn

Received 16 November 2020; Revised 20 January 2021; Accepted 30 January 2021; Published 13 February 2021

Academic Editor: Giovanni Mongelli



A novel density model for computing quartz solubility in $H_2O$-$CO_2$-NaCl hydrothermal fluids applicable to wide ranges of temperature and pressure is proposed. Based on the models of Akinfiev and Diamond (2009) and Wei et al. (2012), the effective partial molar volume of water ($V^*_{H_2O}$) is replaced by the partial molar volume of water ($\bar{V}_{H_2O}$) by implementing an empirical correction, and water molar fraction ($x_{H_2O}$) is modified with water activity ($a_{H_2O}$), in addition to a series of changes to the model coefficient forms. The absolute values of averaged relative deviation of this model compared to the experimental data sets in pure water, $H_2O$-$CO_2$, and $H_2O$-NaCl solutions are 5.74%, 6.69%, and 7.09%, respectively, which are better than existing models in the literature. The model can be reliably used for computing quartz solubilities in pure water from 0°C to 1000°C, from 0 bar to 20,000 bar, and in $CO_2$- and/or NaCl-bearing solutions from 0°C to 1000°C, from 0 bar to 10,000 bar (with slightly lower accuracy at 5000-10,000 bar in $H_2O$-NaCl systems) in the single liquid region. Moreover, the trends and overall ranges of this model may probably be more accurate in the $H_2O$-$CO_2$-NaCl fluid mixtures compared to the limited experimental data. In addition, a bisection algorithm for deriving the isopleths of quartz solubilities based on this new model is first proposed, and application perspectives are discussed for various geologic settings including subduction zone, lower crust-upper mantle, migmatite, pegmatite, porphyry, and orogenic deposits.

## 1. Introduction

Quartz is one of the most common silicate minerals in the Earth's crust. Its solubility behavior in hydrothermal fluids bears fundamental fingerprints on geochemical and petrological processes that govern the formation and evolution of the Earth [1]. For instance, a complete body of knowledge on quartz dissolution and precipitation in crustal fluids is critical for understanding ore-forming processes [2–4]. Particularly, combined with the scanning electron microscope- (SEM-) cathodoluminescence (CL) petrographic technique, formation of quartz veins and veinlets in mineral ore deposits have been intensively studied and better understood due to progressive improvement of solubility models [5–8].

In general, there are two means of deriving quartz solubilities in aqueous fluids, i.e., by hydrothermal experiments and by formulating numerical models. Starting with Kennedy [9], early experiments [10–18] were carried out in pure water and reviewed by Walther and Helgeson [19]. Since the electrolyte (e.g., NaCl) and the nonpolar gas $CO_2$ are very common in various hydrothermal environments and may also play important roles in quartz solubilities [20–24], later the experiment were extended to $H_2O$-NaCl [20, 21, 24–28], $H_2O$-$CO_2$ [20, 21, 26, 29], and $H_2O$-$CO_2$-NaCl [22] fluid mixtures. Meanwhile, higher temperature-pressure ($T$ - $P$) conditions in pure water have been attempted [23, 30–32].

In numerical modeling, there are mainly two types of models: one is "electrostatic model" accounting for the electrostatic interactions between aqueous species and surrounding $H_2O$ molecules [19, 33, 34]; the other is "density model" which is based on the empirical observations and shown as the linear relationship between the decadic logarithm of quartz solubility and the density of

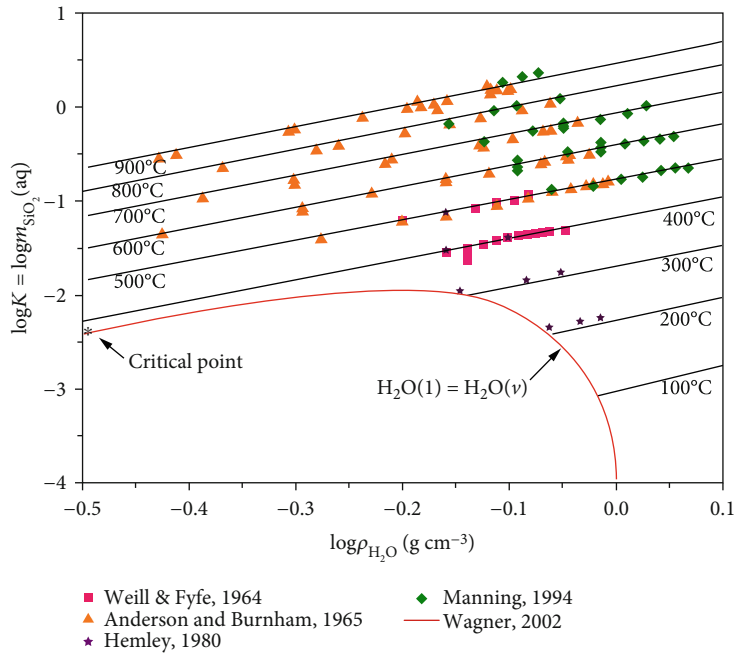


FIGURE 1: Log$m_{SiO_2}$ versus log $\rho_{H_2O}$ for experimental studies and model predictions of quartz solubility at isothermal conditions in pure water. Square, triangle, star, and diamond represent experimental data, and the asterisk is the critical point of $H_2O$. The curve refers to the saturation vapor pressure of $H_2O$, which is calculated from Wagner and Pruß [45], and the solid lines are log $m_{SiO_2}$ calculated from this model.

pure water [2, 30, 35–38]. Due to a lack of knowledge on water dielectric constants at high pressures, electrostatic models are commonly limited pressures less than 5000 bar. Absence of such pressure limitation for density models in addition to their simplicity makes them more powerful and attractive [35–37].

To some extents, the quartz solubilities in hydrothermal fluids and as such them isopleths control the transport and deposition of silica in association with metals and sulfides. Monecke et al. [39, 40] and Li et al. [41] have constructed the quartz isopleths to illustrate the formation of copper- and gold-bearing quartz vein(let)s in porphyry Cu and orogenic Au deposits by calculating large numbers of quartz solubilities along a closely spaced isochores and importing them into the graphing and data analysis software Origin. For one thing, the previous density models for computing quartz solubility either have narrow applicability in fluid systems (such as the model of Manning [30] which is only suitable for pure water and the models of Fournier [2] and Brooks and Steele-MacInnis [38] which are only valid for saline aqueous fluids), limited accuracies in aqueous NaCl and/or $CO_2$ solutions (such as the models of Akinfiev and Diamond [35] and Wei et al. [36] which overestimate quartz solubilities in NaCl-bearing solutions and underestimate quartz solubilities in $CO_2$-bearing solutions), or yield inconsistent results for $H_2O$-$CO_2$-NaCl solutions (model prediction of Shi et al. [37] shows quartz solubility has enhanced follows the gradually adding of $CO_2$ with the same NaCl contents). For another, a convenient and practical method for quartz solubility isopleths is needful. So, a new accurate density model for the solubilities of quartz in $H_2O$-$CO_2$-NaCl fluid mixtures and a simple generic algorithm to get quartz solubility isopleths are necessitated.

The objective of this work is to develop a density model to calculate quartz solubility in $H_2O$-$CO_2$-NaCl hydrothermal solutions cover a wide temperature-pressure-composition ($T$ - $P$ - $x$) range at higher accuracy. Furthermore, an algorithm for acquiring quartz solubility isopleths based on this new model is designed to facilitate applicability. The model here is based on the models of Akinfiev and Diamond [35] and Wei et al. [36] with three revises: introduction of the partial molar volume of water ($\bar{V}_{H_2O}$) for the effective partial molar volume of water ($V^*_{H_2O}$), replacement of water molar fraction ($x_{H_2O}$) by water activity ($a_{H_2O}$), and coefficient form modifications. Detailed modeling process, algorithm on acquiring isopleths, and an applicable case study on quartz solubility isopleths are proposed in the following text.

## 2. Density Model of Quartz Solubility in $H_2O$-$CO_2$-NaCl Solutions

*2.1. Existing Models.* Compared to the experimental ways of knowing quartz solubilities, the numerical models have broader range of application. Early efforts on density modeling were mostly focused on pure water [9, 12, 14, 18, 19, 23, 30, 42–44]. They were established mainly on empirical observations on the logarithm linear relationship between quartz solubility and the density of pure water at constant temperatures (Figure 1). With the accumulation of experimental data, density models have been expanded to gas- and/or salt-bearing solutions. The first of these density models which could be applied to $H_2O$-$CO_2$-NaCl ternary system was

proposed by Shmulovich et al. [22]. Later, Akinfiev and Diamond [35] developed a simple predictive model (thereafter abbreviated as AD 2009 model) based on calculating the effective partial molar volume of water ($V^*_{H_2O}$). With a new form of hydration number, Wei et al. [36] improved the accuracy of AD 2009 model, especially when applied to $H_2O$-NaCl system at high temperatures, pressures, and high NaCl concentrations and proposed a revised model (thereafter abbreviated as WDM 2012 model). Just recently, an accurate density-based model for quartz solubility in aqueous NaCl and/or $CO_2$ solutions was established by Shi and coworkers (thereafter abbreviated as SMH 2019 model [37]). However, the accuracy of SMH 2019 model in $H_2O$-$CO_2$-NaCl fluid mixtures can be further improved as is demonstrated later in Section 4.2.

All the density models for quartz solubility were based on its dissolution and precipitation reaction as the following expression:

$$SiO_{2(quartz)} + n \cdot H_2O \rightleftharpoons SiO_2 \cdot (H_2O)_{n(aq)}. \quad (1)$$

Here, $n$ represents the average number of water molecules complexed with one $SiO_{2(quartz)}$ molecule in an aqueous solution, and $SiO_2 \cdot (H_2O)_{n(aq)}$ stands for the aqueous silica abbreviated as $SiO_{2(aq)}$. For pure quartz, if adopting standard states of unit activity at any temperatures and pressures, the equilibrium constant ($K$) for the above reaction is as follows:

$$\log K_{(1)} = \log \left(a_{SiO_{2(aq)}}\right) - n \cdot \log \left(a_{H_2O}\right), \quad (2)$$

where $a_{SiO_{2(aq)}}$ is the activity of aqueous silica and $a_{H_2O}$ is the activity of pure water. As an approximation, assuming the ideal behavior of $SiO_{2(aq)}$, Eq. (2) could be changed to the following form:

$$\log \left(m_{SiO_{2(aq)}}\right) = \log K_{(1)} + n \cdot \log \left(a_{H_2O}\right), \quad (3)$$

where $m_{SiO_{2(aq)}}$ is the molality of $SiO_{2(aq)}$. Mainly on the empirical observations, more than half a century ago, scientists have noticed that the logarithm of equilibrium constant ($\log K$) for the ionization of water and a variety of aqueous species are linear in the logarithm of the density of pure water ($\log \rho_{H_2O}$) as Figure 1 depicts [30, 46–49], and the correlation for the ionization of $H_2O$ up to 1000°C and 10,000 bar was first proposed by Marshall and Franck [50] with the following equation:

$$\log K = \left(\frac{a+b}{T} + \frac{c}{T^2} + \frac{d}{T^3}\right) + \left(e + \frac{f}{T} + \frac{g}{T^2}\right) \log \rho_{H_2O}, \quad (4)$$

where $a$ to $g$ are the regressed constants and $T$ is temperature in Kelvin (note: all the temperatures in the following equations are in Kelvins unless a description).

Adopting the rapid-quench method, Manning [30] doubled the pressure range which $m_{SiO_{2(aq)}}$ experimental measured and combined the measurements of Hemley et al. [51] and Walther and Orville [29], and he regressed the constants $a$ through $g$ for $SiO_{2(aq)}$ and proposed a successful density model (thereafter abbreviated as M 1994 model) for quartz solubility computing in pure water. Because of its simple form and accuracy, Eq. (4) became a successful density model for calculating quartz solubility in pure water over a wide range of temperatures and pressures (from 25°C and 1 bar to 1000°C and 10,000 bar).

With the activity of a constituent relative to unit activity in an arbitrary standard state, Fournier [2] proposed a method to calculate quartz solubility in aqueous NaCl solutions by modifying his solubility model in pure water. As quartz dissolved in salt-bearing solutions with the form of reaction (1), Fournier [2] started from Eq. (3) and gave his model (thereafter abbreviated as F 1983 model) to compute quartz solubility in NaCl solutions:

$$\log \left(m_{SiO_{2(aq)}}\right) = \log \left(m^o_{SiO_{2(aq)}}\right) + n \log \left(\frac{\rho_e}{\rho^o_e}\right), \quad (5)$$

where $m_{SiO_{2(aq)}}$ and $m^o_{SiO_{2(aq)}}$ are silica solubility in NaCl solutions and in pure water, respectively. In Eq. (5), $\rho_e$ and $\rho^o_e$ are defined as the effective density of "free water" which are not tightly bound to hydrations in NaCl solutions and in pure water (Stokes and Robinson [52]).

Adopted the same dissolution form of Eq. (1) and built on the models of F 1983 and M 1994, Akinfiev and Diamond [35] first proposed a density model (AD 2009 model) to calculate quartz solubility in water-salt-$CO_2$ systems over a broad $T$ - $P$ conditions with the following form:

$$\log m_{SiO_{2(aq)}} = A(T) + B(T) \cdot \log \left(\frac{M_{H_2O}}{V^*_{H_2O}}\right) + 2 \log x_{H_2O}, \quad (6)$$

where $A(T)$ and $B(T)$ are $(a + b/T + c/T^2 + d/T^3)$ and $(e + f/T + g/T^2)$ of the Eq. (4), $M_{H_2O} = 18.0152\,\mathrm{g\,mol^{-1}}$ is the molar mass of water, and $x_{H_2O}$ denotes the mole fraction of water in the mixed fluid. The AD 2009 model introduced a new parameter of "effective partial molar volume of water" ($V^*_{H_2O}$), which is obtained from the relationship below.

$$V^{mol}_{mix} = x_{H_2O} V^*_{H_2O} + x_{NaCl} V_{NaCl} + x_{CO_2} V_{CO_2}, \quad (7)$$

where $V^{mol}_{mix}$ is the molar volume of fluid mixture and $x_{NaCl}$ and $x_{CO_2}$ are the molar fractions of the solute NaCl and $CO_2$. $V_{NaCl}$ and $V_{CO_2}$ are intrinsic volumes of NaCl and $CO_2$, which are the only empirical parameters of AD 2009 model and are derived from experimental data sets of quartz solubilities in $H_2O$-NaCl and $H_2O$-$CO_2$ systems, respectively.

Although AD 2009 model was very successful, however across the whole temperature and pressure spectrum of their model, the solvation number was simply fixed to 2, and this

might be the reason for their model make overestimations in $H_2O$-NaCl mixed fluids over 600°C and 9000 bar conditions (their Figure 5 of Akinfiev and Diamond [35]).

Based on the in situ Raman spectroscopic measurements of aqueous silica in equilibrium with the solid quartz, it was confirmed that the silica speciation depends strongly on temperatures and pressures (Zotov and Keppler [53]). So, the model of Wei et al. [36] was based on the master equation of AD 2009 model but changing the solvation number of aqueous silica complex into a temperature-dependent polynomial $C(T)$ and obtained quartz solubility in $H_2O$-$CO_2$-NaCl ternary hydrothermal solutions. It expressed as the following equation:

$$\log m_{SiO_{2(aq)}} = A(T) + B(T) \cdot \log\left(\frac{M_{H_2O}}{V^*_{H_2O}}\right) + C(T) \log x_{H_2O}. \tag{8}$$

Accordingly, WDM 2012 model revised the overestimates of AD 2009 model in low-moderate NaCl-bearing solutions ($x_{NaCl} < 0.3$), but it is subject to underestimate the molality of aqueous silica in high-salinity solutions compared to the experimental data sets (their Figure 5 of Wei et al. [36]).

Recently, based on the pressure-volume-temperature-composition ($PVTx$) model of Mao et al. [54] and a systematically review of experimental data sets of quartz solubilities, an improved density model for quartz solubility was derived by Shi et al. [37] (SMH 2019 model) as the relationship below:

$$\log m_{SiO_{2(aq)}} = \log K + n \log \rho_{sol} F + \phi_{SiO_2-H_2O}, \tag{9}$$

where $\rho_{sol}$ and $F$ are the density of solution and the mass fraction of water, respectively, and $\phi_{SiO_2-H_2O}$ is the ratio of the activity coefficient of water corresponding to their concentrations with the power of hydration number and the activity coefficient of aqueous $SiO_2$. Although the SMH 2019 model shows excellent performance in pure water and the binary fluid system, its prediction in aqueous NaCl- and $CO_2$-bearing solutions still lacks versatile evaluation, which will be discussed below.

*2.2. New Density Model and Its Parameterization.* The first step of this modelling work is a systematic and comprehensive review of existing experimental data of quartz solubility. As early as 1935, researchers had carried out experimental studies and those measurements had covered $H_2O$, $H_2O$-$CO_2$, $H_2O$-NaCl, and $H_2O$-$CO_2$-NaCl hydrothermal solutions (Table 1). In constant regression, we use parts of experimental data (data with superscripts in Table 1), and others were either some of what unreliable or used as the testing of model prediction. The select regulation of experimental data for regression is basically like the former researchers discussed, and all the detailed information of data selection is listed in our Supplementary A. (Manning [30]; Shi et al. [37]; Fournier and Potter II [43]).

Then, this model is also built on the equilibrium reaction of Eq. (1) and assumes ideal behavior for $SiO_{2(aq)}$ (Eq. (3)), as the empirical expression of the logarithm of the equilibrium constant for aqueous silica is linear with the logarithm of the density of pure water (Eq. (4)) written as follows:

$$\begin{aligned}\log m_{SiO_{2(aq)}} = {} & A(T,P) + B(T,P) \\ & \cdot \log\left(\frac{M_{H_2O}}{\bar{V}_{H_2O}} \cdot \phi\left(T,P,x_{NaCl},x_{CO_2}\right)\right) \\ & + n\left(T,P,x_{NaCl},x_{CO_2}\right) \cdot \log a,\end{aligned} \tag{10}$$

where $\bar{V}_{H_2O}$ is the partial molar volume of water, $M_{H_2O}/\bar{V}_{H_2O}$ refers to the density of pure water in $H_2O$-$CO_2$-NaCl ternary fluid mixtures, and $\phi(T,P,x_{NaCl},x_{CO_2})$ is an empirical parameter on $T$, $P$, $x_{NaCl}$, and $x_{CO_2}$ dependent, which corrects the deviation of the density of "pure water" and the effective density of "free water" (water not tightly bound as water of hydration) as introduced by Fournier [2]. $A(T,P)$ and $B(T,P)$ are $T$ - $P$ dependent polynomials in Kelvins and bars, respectively (note: all the pressures in the following equations are in bars unless a description), and $n(T,P,x_{NaCl},x_{CO_2})$ is the hydration number and as an empirical polynomial expressed with the parameters of $T$, $P$, $x_{NaCl}$, and $x_{CO_2}$. $a_{H_2O}$ is the activity of pure water in $H_2O$-$CO_2$-NaCl solutions which is calculated from the model of Dubacq et al. [66].

In this model, the polynomials of $A(T,P)$, $B(T,P)$, $\phi(T,P,x_{NaCl},x_{CO_2})$, and $n(T,P,x_{NaCl},x_{CO_2})$ are assumed as follows:

$$A(T,P) = A_0 + A_1 T + A_2 T^2 + A_3 T^3 + A_4 T^4 + A_5 P + A_6 P^2 + A_7 P^3, \tag{11}$$

$$B(T,P) = B_0 + B_1 T + B_2 T^2 + B_3 \log P + B_4 (\log P)^2, \tag{12}$$

$$\phi\left(T,P,x_{NaCl},x_{CO_2}\right) = 10^{\left(\left(C_0+C_1T+C_2T^2+C_3P+C_4P^2+C_5x_{NaCl}+C_6x_{NaCl}^2\right)x_{NaCl}+\left(D_0+D_1T+D_2P+D_3P^2+D_4x_{CO_2}\right)x_{CO_2}+F_0x_{NaCl}x_{CO_2}^2\right)}, \tag{13}$$

$$n\left(T,P,x_{NaCl},x_{CO_2}\right) = 2 + \left(N_{00} + N_{01}T + N_{02}T^2 + N_{03}x_{NaCl}^2\right)x_{NaCl} + \left(N_{10} + N_{11}P + N_{12}x_{CO_2} + N_{13}x_{CO_2}^2\right)x_{CO_2}. \tag{14}$$

Table 1: Experimental measurements for quartz solubility.

| Pure $H_2O$ | | | | |
|---|---|---|---|---|
| References | $T$ (K) | $P$ (bar) | | $N_d$ |
| Van Nieuwenburg and Van Zon [55] | 653.15-698.15 | 289.2-490.2 | | 18 |
| Kennedy [9]● | 433.15-883.15 | 6.2-1750 | | 106 |
| Morey and Hesselgesser [10]● | 633.15-873.15 | 33-2000 | | 20 |
| Fournier [56] | 438.15-513.15 | 7-33.5 | | 3 |
| Kitahara [11] | 473.15-643.15 | 15.5-210.4 | | 8 |
| Van Lier et al. [12]* | 333.15-373.15 | 0.2-1.0 | | 5 |
| Morey et al. [13]● | 318.15-573.15 | 0.29-1013.3 | | 51 |
| Siever [14]● | 398.15-454.65 | 2.32-10.4 | | 16 |
| Weill and Fyfe [15] | 673.15-898.15 | 1000-4000 | | 48 |
| Anderson and Burnham [16] | 773.15-1173.15 | 1000-9850 | | 79 |
| Anderson and Burnham [17]* | 973.15 | 4000 | | 2 |
| Crerar and Anderson [18]● | 452.15-602.15 | 9.8-126.9 | | 31 |
| Novgorodov [26] | 973.15 | 1500 | | 1 |
| Hemley et al. [51] | 473.15-773.15 | 15.5-2000 | | 18 |
| Fournier et al. [27]* | 623.15 | 165-500 | | 5 |
| Anderson and Burnham [57] | 773.15-973.15 | 2000-8410 | | 29 |
| Ragnarsdottr and Walther [58] | 523.15 | 250-1000 | | 7 |
| Walther and Orville [29]● | 623.15-823.15 | 1000-2000 | | 20 |
| Archer [59] | 473.15-593.15 | 61-1000 | | 16 |
| Xie and Walther [28] | 685.15-846.15 | 2000-2005 | | 7 |
| Manning [30]● | 773.15-1173.15 | 5000-20,000 | | 52 |
| Rimstidt [60]● | 294.15-369.15 | 0.02-0.88 | | 10 |
| Newton and Manning [20]● | 873.15-1123.15 | 2000-10,000 | | 8 |
| Shmulovich et al. [21]● | 773.15-1173.15 | 5000-9000 | | 7 |
| Wang et al. [61] | 399.15-643.15 | 800-6100 | | 84 |
| Shmulovich et al. [22]● | 673.15-1073.15 | 1000-9000 | | 19 |
| Newton and Manning [31] | 1023.15-1403.15 | 10,000 | | 7 |
| Manning et al. [32] | 573.15-908.15 | 10,000 | | 9 |
| Hunt and Manning [23] * | 1173.15-1323.15 | 15,000-20,000 | | 5 |
| $H_2O$-$CO_2$ mixture | | | | |
| References | $T$ (K) | $P$ (bar) | $x_{CO_2}$ | $N_d$ |
| Novgorodov [26] | 973.15 | 1500 | 0.05-0.49 | 4 |
| Walther and Orville [29]* | 873.15 | 2000 | 0.023-0.31 | 7 |
| Newton and Manning [20]* | 1073.15 | 10,000 | 0.19-0.68 | 5 |
| Shmulovich et al. [21]* | 1073.15 | 9000 | 0.16-0.50 | 5 |
| Shmulovich et al. [22]* | 773.15-1073.15 | 2000-9000 | 0.06-0.50 | 26 |
| Newton and Manning [62]* | 1073.15 | 10,000 | 0.08-0.93 | 14 |
| $H_2O$-NaCl mixture | | | | |
| References | $T$ (K) | $P$ (bar) | $X_{NaCl}$ | $N_d$ |
| Van Lier et al. [12]* | 333.15 | 1.0 | 0.0002 | 11 |
| Anderson and Burnham [17] | 873.15 | 3000 | 0.016 | 1 |
| Ganeyev [25]* | 523.15-773.15 | 1000 | 0.03-0.08 | 17 |
| Novgorodov [26] | 973.15 | 1500 | 0.02-0.13 | 5 |
| Hemley et al. [51]* | 473.15-673.15 | 1000 | 0.009-0.067 | 6 |
| Fournier et al. [27]* | 623.15 | 180-525 | 0.035-0.067 | 35 |

Table 1: Continued.

| | | | | | |
|---|---|---|---|---|---|
| Von Damm et al. [44]* | 472.15-726.55 | | 192-1033 | 0.009 | 100 |
| Xie and Walther [28]* | 675.15-868.15 | | 1725-1800 | 0.0018 | 9 |
| Newton and Manning [20]* | 773.15-1173.15 | | 2000-15,000 | 0.06-0.76 | 50 |
| Shmulovich et al. [21]* | 773.15-1073.15 | | 5000-9000 | 0.02-0.55 | 14 |
| Shmulovich et al. [22]* | 673.15-1073.15 | | 1000-9000 | 0.004-0.55 | 44 |
| Newton and Manning [63]* | 1073.15 | | 10,000 | 0.17 | 1 |
| Foustoukos and Seyfried Jr [64]* | 638.15-703.15 | | 219-378 | 0.0002-0.01 | 92 |
| Cruz and Manning [24]* | 1173.15-1373.15 | | 15,000-20,000 | 0.05-0.5 | 27 |
| Scheuermann et al. [65] | 693.15 | | 310-325 | 0.027-0.046 | 4 |
| $H_2O$-$CO_2$-NaCl mixture | | | | | |
| Reference | $T$ (K) | $P$ (bar) | $x_{CO_2}$ | $X_{Nacl}$ | $N_d$ |
| Shmulovich et al. [22] | 1073.15 | 5000 | 0.07-0.30 | 0.0036-0.25 | 14 |

Note: $N_d$ means the number of measurements. Superscripts * and • denote whole or parts of the experimental data sets which involved in constants regressions, respectively.

By adopting the regressed constants $A_0$ to $A_7$ through $B_0$ to $B_4$ in pure water and by combining the constants $N_{00}$ to $N_{03}$, $N_{10}$ to $N_{13}$, $C_0$ to $C_6$, $D_0$ to $D_4$, and $F_0$ based on regressing quartz solubility data in $H_2O$-NaCl, $H_2O$-$CO_2$, and $H_2O$-$CO_2$-NaCl solutions, the regressed constants of this model are given in Table 2.

For one molar homogenous system which is composed of $H_2O$, NaCl, and $CO_2$, the extensive property of the molar volume of $H_2O$-$CO_2$-NaCl mixture solution $V_{mix}$ could be expressed as the following equation:

$$V_{mix} = \bar{V}_{H_2O} \cdot x_{H_2O} + \bar{V}_{NaCl} \cdot x_{NaCl} + \bar{V}_{CO_2} \cdot x_{CO_2}, \quad (15)$$

where $\bar{V}_{H_2O}$, $\bar{V}_{NaCl}$, and $\bar{V}_{CO_2}$ defined as the "partial molar volume" of $H_2O$, NaCl, and $CO_2$, respectively. At the same time, $V_{mix}$ also can be obtained by the function of Mao et al. [54] as the following form:

$$V_{mix} = V_{mix}\left(T, P, x_{NaCl}, x_{CO_2}\right). \quad (16)$$

Based on the definition of the partial molar volume, $\bar{V}_{NaCl}$ and $\bar{V}_{CO_2}$ at constant $T$ and $P$ can be further written as follows:

$$\bar{V}_{NaCl} = \left(\frac{\partial V_{mix}}{\partial x_{NaCl}}\right)_{T,P}, \quad (17)$$

$$\bar{V}_{CO_2} = \left(\frac{\partial V_{mix}}{\partial x_{CO_2}}\right)_{T,P}. \quad (18)$$

If $V_{mix}$ is continuous differentiable in a closed interval of $[x_i, x_i + \Delta h]$ ($x_i$ means the molar fraction of NaCl or $CO_2$ solute at any fixed $T$ and $P$ conditions, and $\Delta h$ is an incremental change of the molar fraction of NaCl or $CO_2$ solute), according to the Taylor expansion of $V_{mix}$, it reduces to

$$V_{mix}(x_i + \Delta h) = V_{mix}(x_i) + \Delta h \frac{dV_{mix}(x_i)}{dx_i} + \frac{\Delta h^2}{2}\frac{d^2 V_{mix}(c)}{dx_i^2}, \quad (19)$$

where $c$ is a constant and between $x_i$ and $x_i + \Delta h$, and according to the finite difference method (FDM), Eq. (19) can be transformed into

$$\frac{dV_{mix}(x_i)}{dx_i} = \frac{V_{mix}(x_i + \Delta h) - V_{mix}(x_i)}{\Delta h} - o(\Delta h), \quad (20)$$

where $o(\Delta h)$ is the equivalence infinitesimal of $\Delta h$ and equals to $\Delta h/2(d^2 V_{mix}(c)/dx_i^2)$. In our calculation process when $\Delta h/x$ values $10^{-4}$, the term of $dV_{mix}(x_i)/dx_i$, namely, $\bar{V}_{NaCl}$ or $\bar{V}_{CO_2}$ is solved out.

As Shi and coworkers [37] discussed, when the SMH 2019 model applied to $H_2O$-$CO_2$-NaCl solutions, the part of $\phi^r_{NaCl,CO_2}$ which accounts for the nonadditivity of the contributions of NaCl and $CO_2$ to $\phi_{SiO_2-H_2O}$ is very small and can be neglected in most cases, so in this model, $\bar{V}_{NaCl}$ and $\bar{V}_{CO_2}$ in Eq. (17) and Eq. (18) could be solved out with FDM in $H_2O$-NaCl and $H_2O$-$CO_2$ systems, respectively, and the value of $\bar{V}_{H_2O}$ in Eq. (15) will then be calculated.

*2.3. Accuracy Test of This Model.* The accuracy of this new model is compared with the most competitive three ones, i.e., the AD 2009 model, WDM 2012, model and SMH 2019 model by investigating the absolute values of averaged relative deviations (AARDs) (listed in Table 3) from experimental data over a broad $T$-$P$-$x$ spectrum. For quartz solubilities in $H_2O$, $H_2O$-$CO_2$, and $H_2O$-NaCl solutions, the overall AARDs of this model are 5.74%, 6.69%, and 7.09%,

Table 2: Regressed constants for Eq. (10).

| $A(T,P)$ | Values | $B(T,P)$ | Values | $\Phi(T,P,x_{NaCl},x_{CO_2})$ | Values | $n(T,P,x_{NaCl},x_{CO_2})$ | Values |
|---|---|---|---|---|---|---|---|
| $A_0$ | -9.52462828$E$+00 | $B_0$ | 7.92625728$E$+00 | $C_0$ | 4.83288536$E$-01 | $N_{00}$ | 1.76415897$E$+01 |
| $A_1$ | 2.91941547$E$-02 | $B_1$ | -1.53823138$E$-02 | $C_1$ | -1.32770018$E$-04 | $N_{01}$ | -3.05577769$E$-02 |
| $A_2$ | -4.00569452$E$-05 | $B_2$ | 9.14289810$E$-06 | $C_2$ | 1.12520228$E$-07 | $N_{02}$ | 1.25299576$E$-05 |
| $A_3$ | 2.71067438$E$-08 | $B_3$ | 4.03311251$E$-01 | $C_3$ | 4.07784959$E$-05 | $N_{03}$ | -1.99999983$E$+00 |
| $A_4$ | -6.73901359$E$-12 | $B_4$ | -6.91374075$E$-02 | $C_4$ | -3.13938041$E$-09 | $N_{10}$ | -1.15563053$E$+00 |
| $A_5$ | -1.86478387$E$-06 | | | $C_5$ | -9.00618419$E$-01 | $N_{11}$ | -3.69288750$E$-05 |
| $A_6$ | 4.10234340$E$-10 | | | $C_6$ | 9.50723453$E$-01 | $N_{12}$ | 5.56872025$E$+00 |
| $A_7$ | -1.16951479$E$-14 | | | $D_0$ | -1.72890706$E$+00 | $N_{13}$ | -4.03999992$E$+00 |
| | | | | $D_1$ | 1.41633612$E$-03 | | |
| | | | | $D_2$ | 1.43379216$E$-04 | | |
| | | | | $D_3$ | -7.23903865$E$-09 | | |
| | | | | $D_4$ | 2.32574082$E$+00 | | |
| | | | | $F_0$ | 6.99791510$E$+00 | | |

respectively. Although inferior to the SMH 2019 model in aqueous NaCl solutions, the performance of this model has advantages in aqueous $CO_2$ fluids. In addition, this model has made an obvious progress in pure water and NaCl- and/or $CO_2$-bearing solutions which compared to the AD 2009 model and the WDM 2012 model.

The AARD of this model in pure water is 5.74%, only <50% of that of WDM 2012 and AD 2009, and is smaller than that of the SMH 2019. As can be seen from Figure 2(a), this model can predict the dissolution and precipitation behavior of quartz in pure water over broad $T$ - $P$ conditions (up to 1000°C and 20,000 bar). Two points should be emphasized: first, this model reproduced quartz retrograde phenomenon (quartz increases with decreasing temperature) near the critical point of water at low pressures (200 bar and 500 bar) much more accurate compared to other models discussed here (Figure 2(b)); second, except for the data sets of Manning [30] and parts of Shmulovich et al. [22], the solid curve in Figure 2(c) presented the predictability of this model (for those other data sets were not used in constants regression) and which can be seen that this model had better accuracy compared to other models especially in high pressure conditions (Figures 2(c) and 2(d)).

Comparisons of different models computing and experimental data sets in $H_2O$-$CO_2$ solutions are shown in Table 3 and Figures 3(a) and 3(b). Generally, the calculated results of this model matched the experimental data quite well, and the overall AARD of this model is 6.69% which is about 50% better than that of WDM 2012 and AD 2009 and about 30% better than the model of SMH 2019. As Figure 3(a) depicts, at 500°C, 2000 bar, both WDM 2012 and AD 2009 models underestimate quartz solubility slightly, while SMH 2019 overestimates. The WDM 2012 and AD 2009 models underestimate the quartz solubility at high temperature and moderate pressure at 800°C and 5000 bar, whereas the SMH 2019 model overestimates (note: the circle points in Figure 3(b) are the experimental data at 10,000 bar condition). Though the data themselves are very scattered at 800°C, 5000 bar condition, compared to other models, this model seems better fit. When $x_{CO_2}$ is higher than 0.5 at 800°C, 10,000 bar condition, the WDM 2012 and AD 2009 models underestimate quartz solubility, but the SMH 2019 model overestimates although the data sets of Newton and Manning [62] are as the extrapolation testing for their model (Figure 3(b)). Overall, our model seems to have the best performance under the conditions as Figures 3(a) and 3(b) depict.

Figures 3(c)–3(e) show that this model can reproduce quartz solubility well in aqueous $H_2O$-NaCl solutions and is in good agreement with experimental data sets at most temperature and pressure conditions. After excluding some experimental data sets which inconsistent with themselves or having systematic errors (such as some data of Newton and Manning [20] and Cruz and Manning [24]), the overall AARD of this model is 7.09% (Table 3), which has made big improvement compared to the WDM 2012 model and the AD 2009 model, but little inferior than the SMH 2019 model. At 700°C, 2000 bar, compared to the experimental data points of Newton and Manning [20], this model better reproduced the "salting-in" effect (quartz solubility is enhanced with NaCl content) whereas other models all overestimate as Figure 3(c) depicts. At 800°C, 5000 bar high temperature and moderate pressure condition, the accuracy of this model is almost the same as that of the model SMH 2019 and is obviously better than those of the WDM 2012 and the AD 2009 (Figure 3(d)). As Figure 3(e) depicts at 900°C, 10,000 bar condition, this model overestimates quartz solubility in low NaCl-bearing system whereas gives accurate result in higher $x_{NaCl}$ condition when the pressure is much beyond the applicable limitation of the equation of state (EOS) for $V_{mix}$ calculation from Mao et al. [54]. However, when considering the quartz solubility in pure water at the same $T$, $P$ condition (as the circle point by Manning [30] in Figure 3(e)), this overestimation may not be that "over,"

Table 3: Deviations of calculated values on quartz solubility.

| References | $N_d$ | [1]AARD/% | [2]AARD/% | [3]AARD/% | [4]AARD/% |
|---|---|---|---|---|---|
| Pure $H_2O$ | | | | | |
| Kennedy [9]● | 79 | 4.95 | 5.12 | 7.46 | 6.29 |
| Morey and Hesselgesser [10]● | 10 | 5.66 | 5.46 | 2.56 | 3.39 |
| Kitahara [11] | 6 | 6.37 | 6.44 | 9.51 | 8.92 |
| Van Lier et al. [12]* | 5 | 4.89 | 2.84 | 25.86 | 21.66 |
| Morey et al. [13]● | 32 | 4.98 | 10.96 | 25.35 | 21.90 |
| Siever [14]● | 10 | 6.15 | 7.47 | 16.88 | 13.01 |
| Weill and Fyfe [15] | 37 | 4.27 | 3.67 | 4.75 | 5.69 |
| Anderson and Burnham [16] | 79 | 9.04 | 5.71 | 11.31 | 13.46 |
| Anderson and Burnham [17]* | 2 | 4.27 | 6.21 | 14.81 | 17.13 |
| Crerar and Anderson [18]● | 15 | 7.26 | 9.97 | 13.73 | 11.04 |
| Hemley et al. [51] | 18 | 4.13 | 3.67 | 10.62 | 10.70 |
| Fournier et al. [27]* | 5 | 2.00 | 2.48 | 8.13 | 3.02 |
| Anderson and Burnham [57] | 8 | 7.80 | 7.33 | 9.66 | 11.44 |
| Ragnarsdottr and Walther [58] | 4 | 7.75 | 5.32 | 8.52 | 5.09 |
| Walther and Orville [29]● | 15 | 4.62 | 4.27 | 6.41 | 5.74 |
| Archer [59] | 13 | 8.08 | 30.07 | 35.91 | 33.85 |
| Xie and Walther [28]* | 6 | 10.67 | 12.07 | 13.68 | 13.87 |
| Manning [30]● | 52 | 5.32 | 6.62 | 5.70 | 6.80 |
| Rimstidt [60]● | 10 | 5.37 | 19.48 | 27.44 | 23.24 |
| Newton and Manning [20]● | 8 | 5.29 | 5.46 | 9.74 | 11.13 |
| Shmulovich et al. [21]● | 5 | 6.79 | 9.58 | 6.64 | 8.29 |
| Shmulovich et al. [22]● | 15 | 3.96 | 4.23 | 3.50 | 3.91 |
| Newton and Manning [31] | 3 | 2.62 | 17.13 | 17.16 | 17.03 |
| Hunt and Manning [23]* | 4 | 5.55 | 24.7 | 29.46 | 28.19 |
| Overall AARD/% | | 5.74 | 9.01 | 13.53 | 12.70 |
| $H_2O$-$CO_2$ mixture | | | | | |
| Walther and Orville [29]* | 5 | 2.04 | 2.97 | 6.53 | 7.72 |
| Newton and Manning [20]* | 4 | 7.11 | 9.49 | 14.85 | 15.21 |
| Shmulovich et al. [21]* | 5 | 7.19 | 6.52 | 16.41 | 17.76 |
| Shmulovich et al. [22]* | 20 | 9.22 | 17.18 | 10.52 | 15.64 |
| Newton and Manning [62]* | 9 | 7.90 | 11.43 | 9.38 | 28.62 |
| Overall AARD/% | | 6.69 | 9.52 | 11.54 | 16.99 |
| $H_2O$-NaCl mixture | | | | | |
| Van Lier et al. [12]* | 7 | 8.01 | 14.48 | 33.29 | 29.38 |
| Anderson and Burnham [17] | 1 | 3.22 | 5.77 | 13.30 | 15.36 |
| Ganeyev [25]* | 10 | 14.90 | 15.88 | 16.71 | 20.68 |
| Novgorodov [26] | 5 | 9.84 | 9.11 | 14.75 | 15.19 |
| Hemley et al. [51]* | 3 | 5.54 | 2.08 | 8.53 | 8.34 |
| Fournier et al. [27]* | 35 | 1.38 | 1.58 | 3.63 | 3.66 |
| Von Damm et al. [44]* | 100 | 2.34 | 3.40 | 6.77 | 5.70 |
| Xie and Walther [28]* | 9 | 10.75 | 10.50 | 13.52 | 15.04 |
| Newton and Manning [20]* | 45 | 6.59 | 4.61 | 11.23 | 19.82 |
| Shmulovich et al. [21]* | 12 | 6.86 | 6.44 | 9.40 | 10.50 |
| Shmulovich et al., [22]* | 40 | 7.73 | 5.77 | 9.14 | 8.28 |
| Foustoukos and Seyfried Jr [64]* | 75 | 4.31 | 3.01 | 4.67 | 3.75 |

Table 3: Continued.

| References | $N_d$ | [1]AARD/% | [2]AARD/% | [3]AARD/% | [4]AARD/% |
|---|---|---|---|---|---|
| Cruz and Manning [24]* | 14 | 11.90 | 12.04 | 55.39 | 19.13 |
| Scheuermann et al. [65] | 4 | 5.90 | 2.84 | 3.69 | 4.38 |
| Overall AARD/% | | 7.09 | 6.97 | 14.57 | 12.80 |

Notes: $N_d$ is the number of experimental data points; superscripts * and • denote whole or parts of the experimental data sets which involved in constant regressions, respectively; AARD is the absolute value of averaged relative deviation calculated from models; superscripts 1 to 4 represent the models of this one, the SMH 2019, the WDM 2012, and the AD 2009, respectively.

and the predictions by models of SMH 2019, WDM 2012, and AD 2009 may seem a litter lower.

Till now, only 14 experimental data points of quartz solubility have reported in $H_2O$-$CO_2$-NaCl ternary solution by the work of Shmulovich et al. [22] (at $x_{H_2O} = 0.7$). As seen from Figure 3(f), although the data sets are fairly scattered covering a wide spectrum of $x_{CO_2}$ and $x_{NaCl}$ condition from 0 to 0.3, however all model computing results are between them (after deleting some data points with obvious discrepancy as the open squares in their Figure 6 of Shi et al. [37]). Moreover, only this model can approach both two end-member systems of $H_2O$-$CO_2$ and $H_2O$-NaCl solutions on quartz solubility reproducing. Certainly, this model invites stricter testing by future experimental data sets.

There still some points worth of mentioning for the new model. Firstly, the success of this density model may be derived from the highly accurate EOS for $V_{mix}$ and $a_{H_2O}$ computing and more physically meaning parameters the model having. Secondly, only parts of experimental data sets in pure water (the data with superscriptions in Table 1) were used in the constant regression, so the computing result of the solid curve in Figure 2(c) can represent the prediction of this model to some extent. In addition, although the form of the solvation number $n$ in our model is empirical, it may have a physical explanation of assigning it to fixed 2 in pure water (the fixed value of $n$ is for simplistic in model computing for the contribution from $a_{H_2O}$ on quartz solubility will always be zero in pure water, and it could be seemed as the hydration number only when temperatures and pressures are below 600°C and 6000-8000 bar conditions) or depending on $T$, $P$, $x_{NaCl}$, and/or $x_{CO_2}$ conditions in NaCl and/or $CO_2$-bearing solutions which were verified from in situ Raman spectroscopic study on silica speciation in aqueous fluids depends strongly on $T$, $P$ and the study on silica hydration changing with the fluid adding of NaCl or $CO_2$ species [35, 53]. Besides, we think the form of $n$ in our model may be an empirical way to get hydration number on quartz dissolution in NaCl and/or $CO_2$-bearing fluids but should be carefully treated and tested by more studies on silica molecule structures. Lastly, this model can extrapolate to high temperatures and high pressures within or approaching experimental accuracy (for instance, the absolute value of averaged experimental error from the experimental data of Newton and Manning [31] which is carried in $H_2O$ at 1223.15 K and 10,000 bar condition is 2.91%, and the absolute value of averaged relative deviation calculated from this model is 2.93%), for those conditions are beyond the $T$ - $P$ validation of the EOS computing on $V_{mix}$ obtained from Mao et al. [54] (validated from 273 to 1273 K, from 1 to 5000 bar for the $H_2O$-NaCl system, from 273 to 1273 K, and from 1 to 10,000 bar for the $H_2O$-$CO_2$ system) and $a_{H_2O}$ obtained from Dubacq et al. [66] (validated from 283 to 653 K and from 1 to 3500 bar).

## 3. Algorithm for Determining Solubility Isopleths

*3.1. Design of the Numerical Approach.* Quartz solubility isopleths have been widely used to quantify the magnitudes and trends of quartz solubility. In some recent studies, those isopleths provided critical knowledges for understanding volcanogenic massive sulfide deposits, the porphyry deposits, and the orogenic gold deposits [39–41, 67, 68]. Compared to the ways of Monecke et al. [39, 40] and Li et al. [41] for plotting their isopleths by repeat calculating numerous quartz solubilities (they were with the same method of calculating quartz solubilities along a closely spaced isochores and imported them into the graphing and data analysis software Origin), here, we provide a method to obtain those isopleths by a bisection algorithm which is based on this new model on quartz solubility in hydrothermal fluid mixtures over a broad $T$ - $P$ - $x$ spectrum.

As can be seen from Eqs. (10) and (15) and $a_{H_2O}$ calculated from the model of Dubacq et al. [66], the parameters of this density model are only variables of temperatures, pressures, and fluid compositions. So, this model can be transformed as Eq. (21) and simply expressed as follows:

$$m_{SiO_{2(aq)}} = M_{SiO_{2(aq)}}\left(T, P, x_{NaCl}, x_{CO_2}, x_{H_2O}\right), \quad (21)$$

where $M_{SiO_{2(aq)}}$ is the function of quartz solubility with $T$, $P$, $x_{CO_2}$, $x_{NaCl}$, and $x_{H_2O}$ as variables.

Many experimental studies on quartz solubility have shown that at fixed $T$, $x_{CO_2}$, $x_{NaCl}$, and $x_{H_2O}$ fluid compositions, the quartz solubility $m_{SiO_2}$ for pressures $P$ (below 20,000 bar) is continuous monotonically changed (Figures 2(c) and 2(d)). So, the strategy for computing solubility isopleths is to solve each given $m_{SiO_2}$ quantity with $T$ - $P$ relationships at a fixed composition with a bisection algorithm.

*3.2. Computing Programs.* The above algorithm is embedded in a Fortran program, and the computing procedure is as Figure 4 described. For obtaining one point on quartz

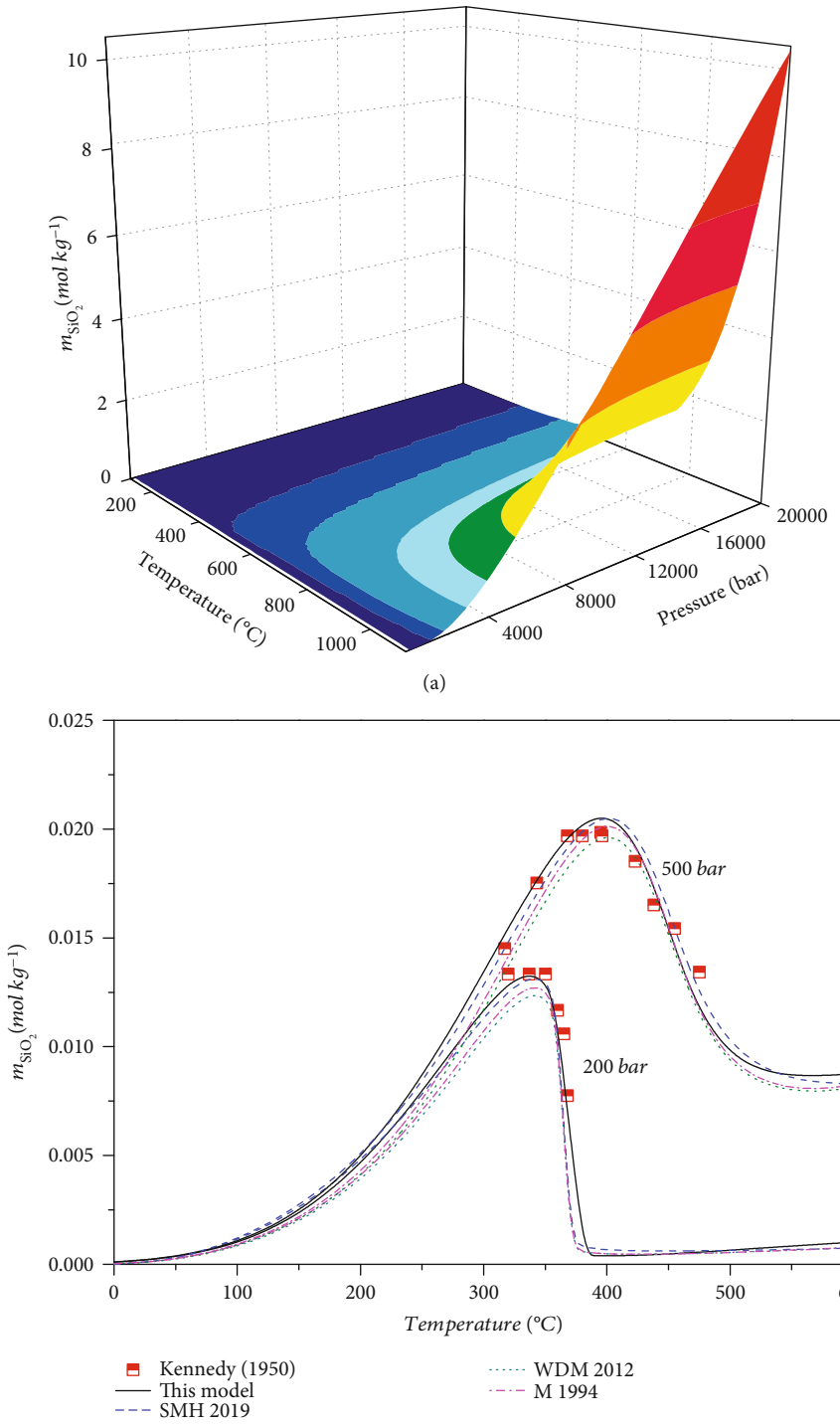


Figure 2: Continued.

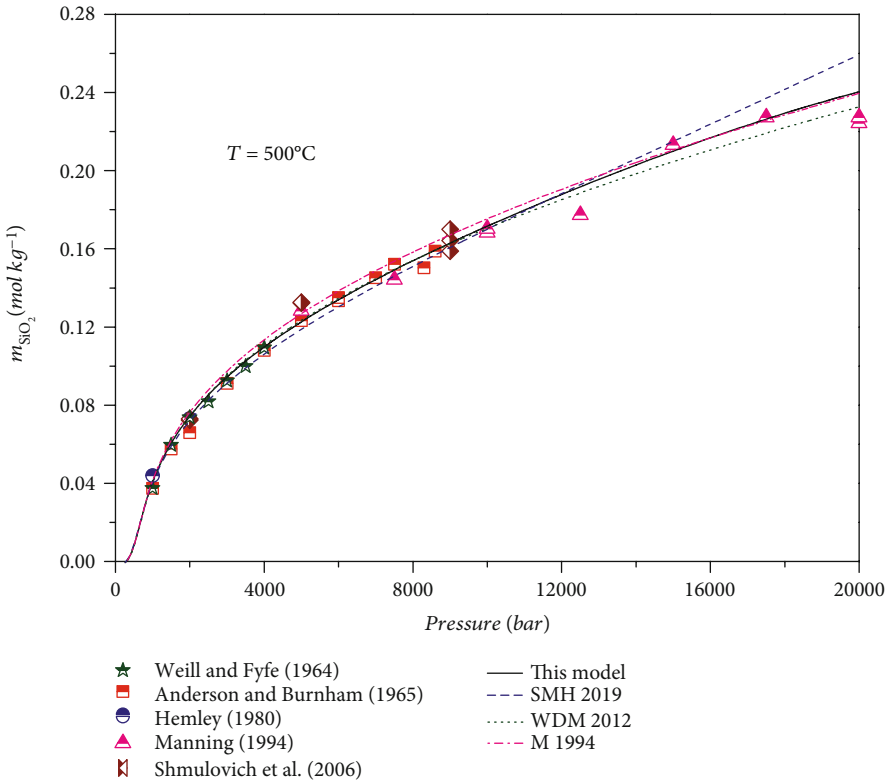


(c)

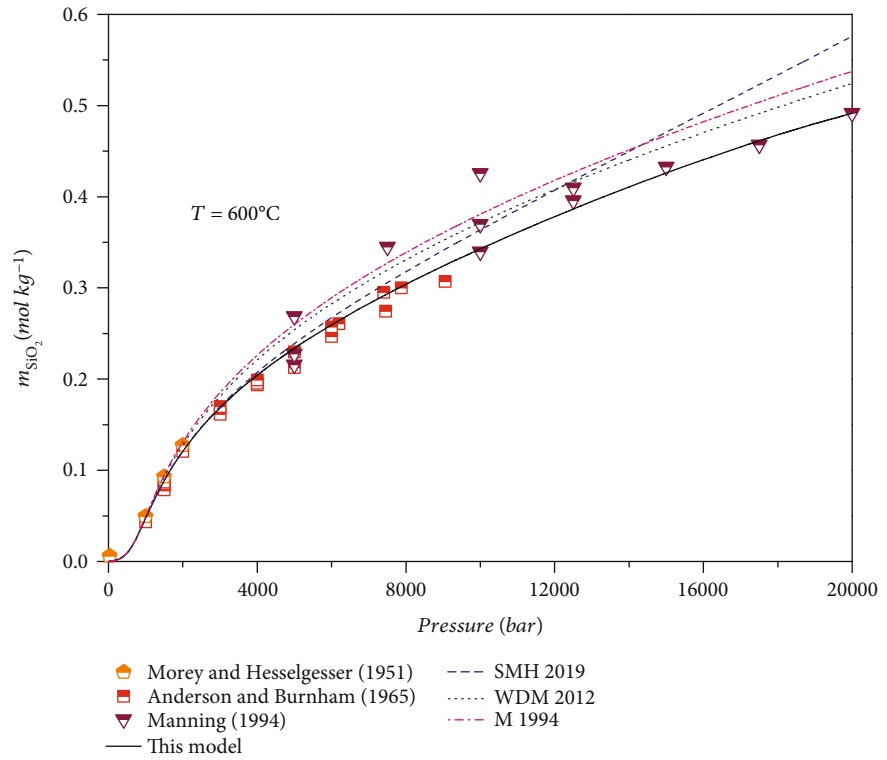


(d)

Figure 2: Model predictions of quartz solubility in pure water and the comparisons between different model computes and experimental data sets. Symbols represent experimental data, and curves are the predictions of different models.

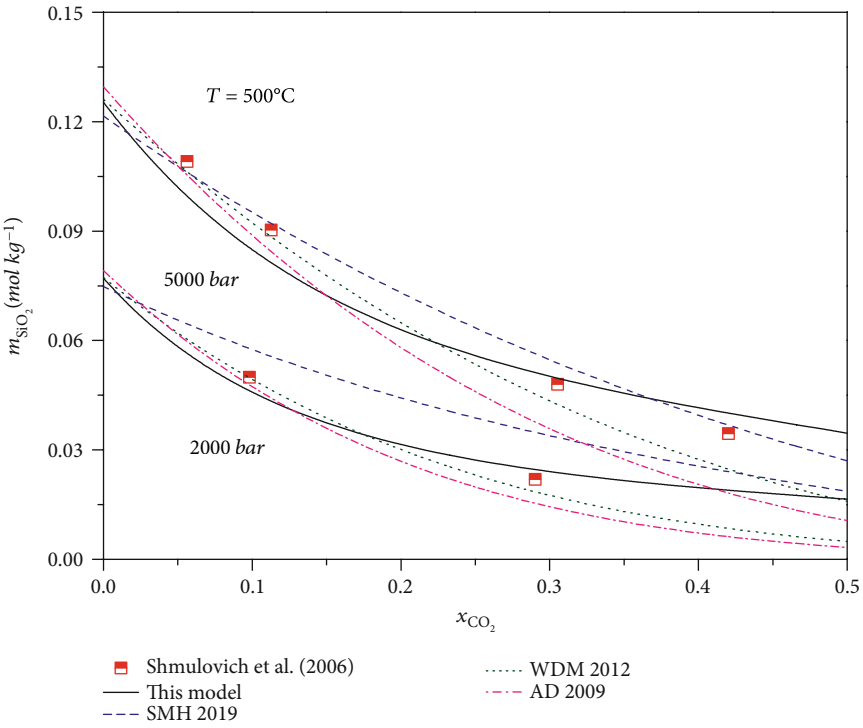


(a)

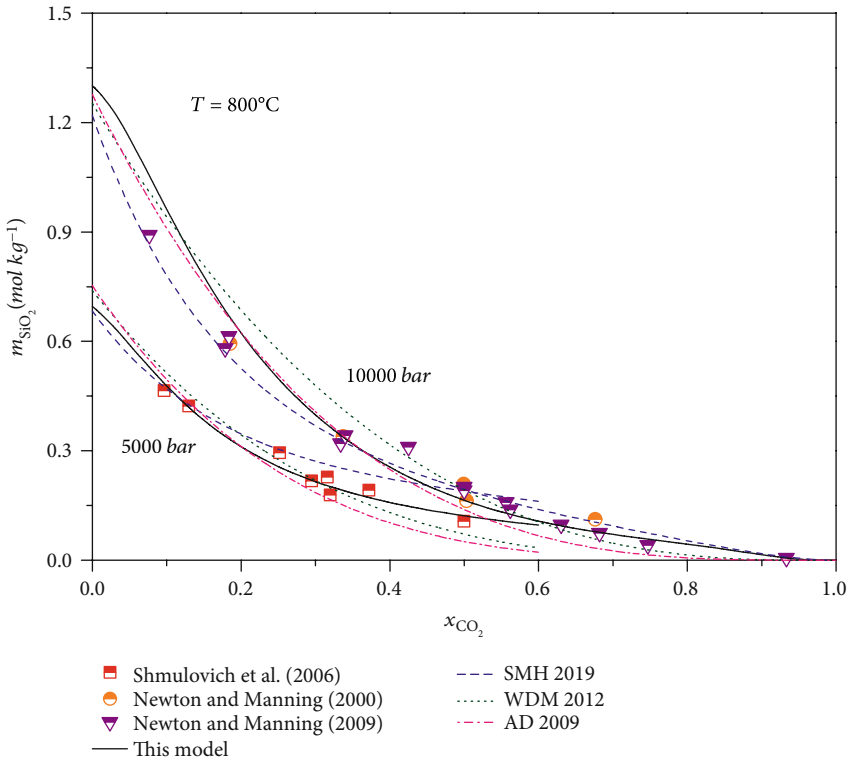


(b)

Figure 3: Continued.

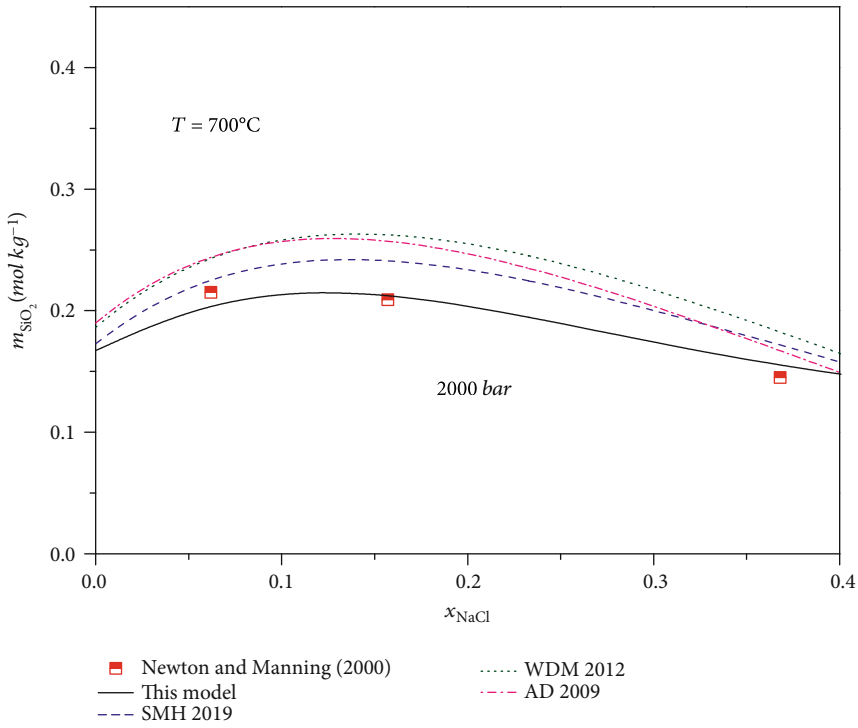


(c)

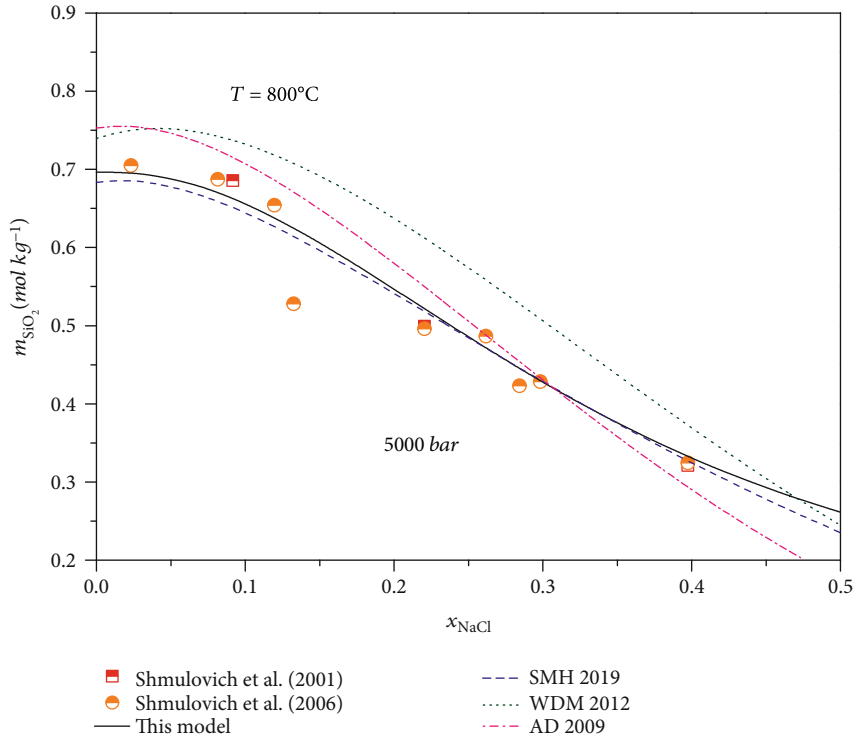


(d)

Figure 3: Continued.

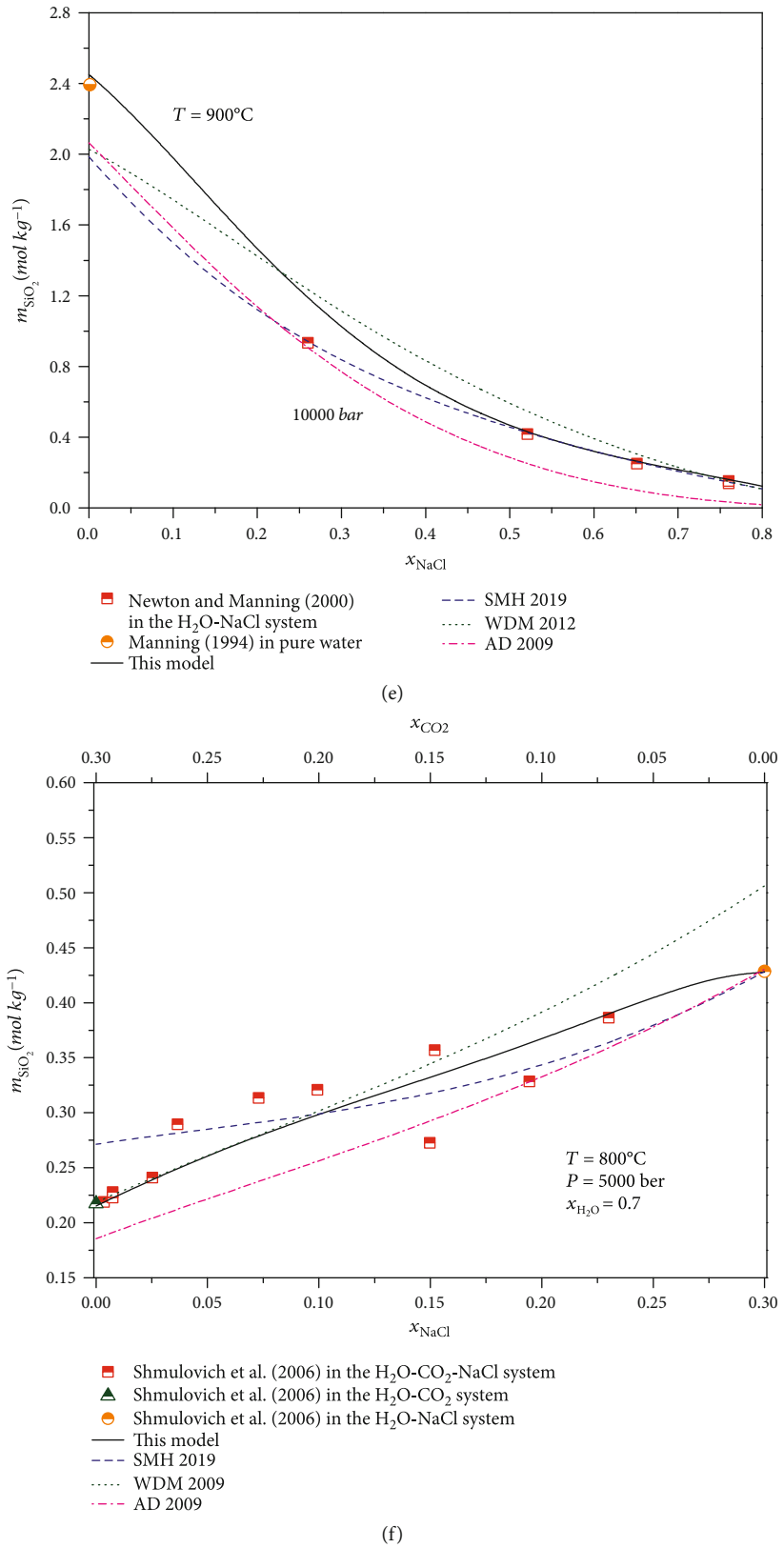


FIGURE 3: Model predictions of quartz solubility in (a, b) aqueous $CO_2$ solutions, in (c–e) aqueous NaCl solutions, and in (f) $CO_2$- and NaCl-bearing solutions. Different curves denote comparisons between four model computes and experimental data sets. Symbols represent experimental data, and curves are the predictions of different models.

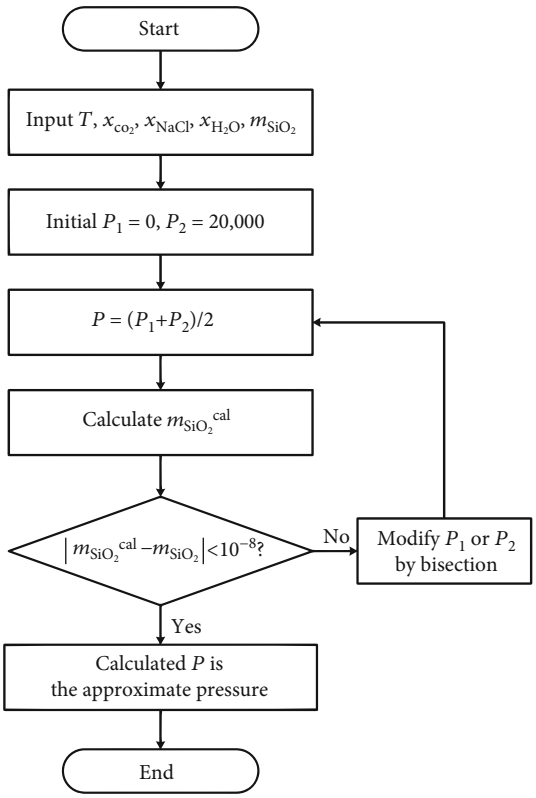


FIGURE 4: A flow chart on bisection algorithm for calculating quartz solubility isopleths in $H_2O$-$CO_2$-NaCl hydrothermal solutions. Parameters *of* $T$, $x_{CO_2}$, $x_{NaCl}$, $x_{H_2O}$, $m_{SiO_2}$, $m_{SiO_2}^{cal}$, $P_1$, and $P_2$ are as defined in the text, respectively.

solubility isopleths (consisting of many points) in the computational steps,

(i) Input parameters $T$, $x_{CO_2}$, $x_{NaCl}$, and $m_{SiO_2}$, in which $T$ is in ˚C (between 0 and 1000˚C) and $m_{SiO_2}$ is in moles per kilogram $H_2O$

(ii) Assume initial boundary pressure $P_1 = 0$ bar and $P_2 = 20{,}000$ bar

(iii) Calculate quartz solubility $m_{SiO_2}^{cal}$ with this density model (Eq. (10)) at $P = (P_1 + P_2)/2$

(iv) Modify $P_1$ or $P_2$ by a bisection method (if $m_{SiO_2}^{cal} < m_{SiO_2}$, then $P_1 = P$; otherwise, $P_2 = P$) and repeat step III until the absolute difference between $m_{SiO_2}^{cal}$ and $m_{SiO_2}$ is less than $10^{-8}$ mol kg$^{-1}$

(v) The calculated $P$ which satisfied the convergence condition is the approximate numerical solution of this program

Please note that the quartz solubility isopleths are sets of $T$ - $P$ relations which are based on recomputing the above program with any interval of temperatures $T$ at fixed $x_{CO_2}$, $x_{NaCl}$, $x_{H_2O}$, and $m_{SiO_2}$ conditions.

*3.3. Application on Isopleths for Single-Phase Region.* Gold mineralization especially for the orogenic intrusion-related gold deposits is dominated by low to intermediate salinity $CO_2$-bearing aqueous solutions and often has embodied themselves on the auriferous quartz veins [4, 39–41, 68]. On the contrary, the $T$ - $P$ - $x$ properties of hydrothermal processes control the type of Au complexing, transport, and deposition in minerals, as well as quartz dissolution and precipitation [41]. Slope patterns of quartz solubility isopleths with different fluid compositions make an insightful way on understanding those veins and even those ores' formation.

An application example on iso-solubility curves in the single liquid region for temperature range of 300 to 500˚C, pressure range 0 to 4000 bars, a fixed salinity of 5 wt. %, and $CO_2$ content ranges of 5 mol % and 15 mol% is acquired based on this new model and the algorithms presented above (Figure 5). These solubility diagrams are designed for orogenic gold systems (for the $T$ - $P$ - $x$ condition designed) but are applicable for all other systems satisfying the physical and chemical conditions mentioned above. The phase boundaries between the single phase and the liquid plus vapor phase in the $H_2O$-$CO_2$-NaCl system are calculated using the model of Mao et al. [69]. The $P$, $T$ ranges of phase boundaries calculating which outside of the applicable range of Mao et al. [69] were extrapolated (model validation is from 273.15 K to 723.15 K and from 1 bar to 1500 bar).

Generally, the regions of isopleths in the diagrams with parallel and gentle slopes mean quartz solubilities are sensitive to the pressure changing, with steep and drastic slopes mean quartz solubilities are sensitive to the temperature changing, and with crossing higher isopleths when temperature is decreasing mean quartz solubilities reflect retrograde features. In the $H_2O$-$CO_2$-NaCl single-phase field of mesothermal gold mineralization concerned with 5 wt. % NaCl and/or 5-15 mol % $CO_2$ containing (Figure 5), it was revealed from this work that quartz solubilities generally not appear retrograde phenomenon and depend strongly on temperature at pressures higher about 1500 bar whereas little on pressure dependences. Isobaric cooling may be the main reason for quartz precipitating. At lower pressures about less than 1500 bar, quartz solubility isopleths are strongly curved with parallel and gentle slopes which means isothermal decompression and isobaric cooling are act together on quartz precipitations. The above conclusions are similar to the systematical research of Li et al. [41] as their Figures 6–8 depict. A noteworthy feature is that this algorithm can also calculate quartz solubility isopleths in liquid plus vapor phase by adding quartz solubility of both phases only if the phase proportion is known [40, 41].

## 4. Discussion

*4.1. Extrapolation to High Temperatures and Pressures.* As discussed in Section 2.3, the limit on temperatures and pressures for this semiempirical thermodynamic model is mainly set by the $PVTx$ model of Mao et al. [54] in addition to the water activity model of Dubacq et al. [66]. However, this model can be used in higher temperature and pressure hydrothermal conditions. For the upper critical endpoint

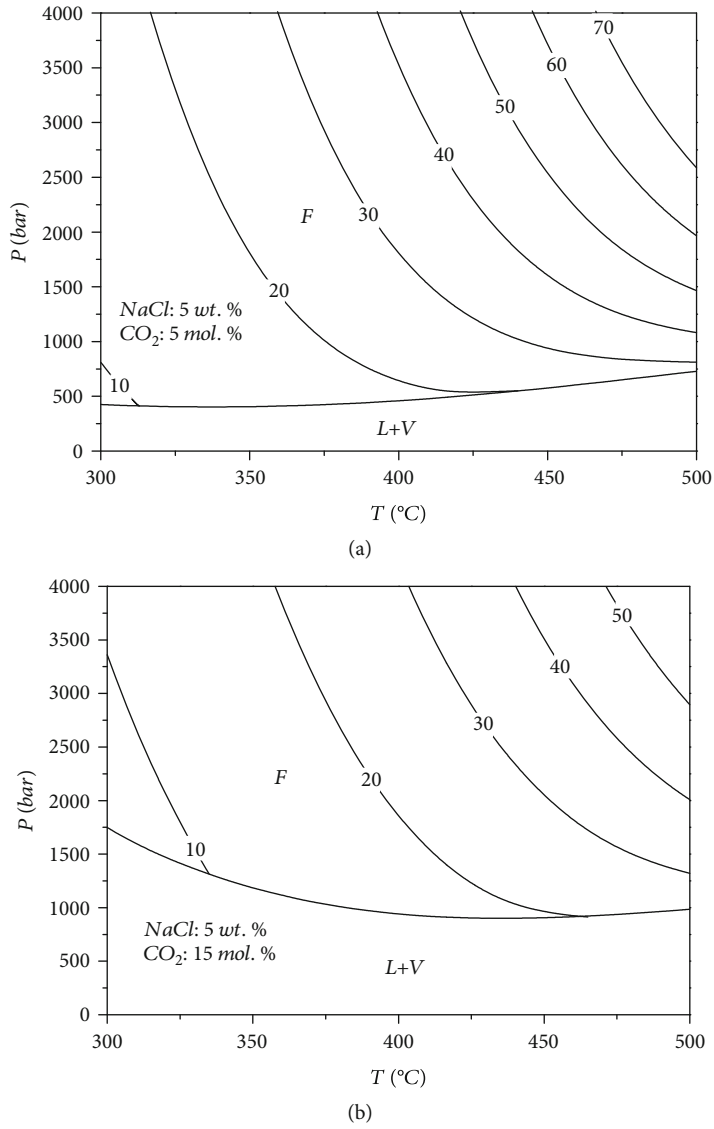


Figure 5: Quartz solubility isopleths in $H_2O$-$CO_2$-NaCl hydrothermal fluids containing the same NaCl contents and different $CO_2$ contents in the single phase which are calculated from this density model and the isopleth algorithm, at 300-500°C and 0.01-4000 bar. (a) 5 wt. % NaCl and 5 mol % $CO_2$ containing. (b) 5 wt. % NaCl and 15 mol % $CO_2$ containing. Quartz solubilities are recorded in millimoles per kilogram $H_2O$. *F*: the single-phase fluid; $L + V$: liquid plus vapor phase fluid. The thin curves represent quartz solubility isopleths, and the thick curves are phase boundaries.

($T = 1353$ K and $P = 9500$-10,000 bar) which Newton and Manning [31] pointed out; although Shi et al. [37] had stated that their model and the models of WDM 2012 and M 1994 are all failure in the $H_2O$-$SiO_2$ system, however, it seems that the present model works better than others on the sharp-enhanced trends of quartz solubility when extrapolated to high temperatures (more than 1000°C) which are shown in Figures 6(a) and 6(b). Summarized in the work of Manning [30], it is convinced that this model can be extrapolated to high pressures (more than 20,000 bar) in pure water which is benefited from the empirical linear relationship between the logarithm of equilibrium constant ($\log K$) for a variety of aqueous and the logarithm of water density ($\log \rho_{H_2O}$), and only parts of experimental data sets were used in constant regression. In $H_2O$-NaCl mixture solutions, the extrapolation ability of this model is obvious enhanced than models of WDM 2012 and AD 2009 as well as is compared to the latest SMH 2019 model at high pressures (Figures 6(c) and 6(d)). We should note that those pressure conditions are far beyond their model application scopes of Mao et al. [54] and Dubacq et al. [66].

*4.2. Prediction in Complex Fluids.* One thing should be mentioned is that this thermodynamic model relies only on few experimental data in the $H_2O$-$CO_2$-NaCl mixtures (Figure 3(f), Shmulovich et al. [22]), which makes it difficult on model predictions in the above ternary system. The SMH 2019 model has adopted the solubility experimental data

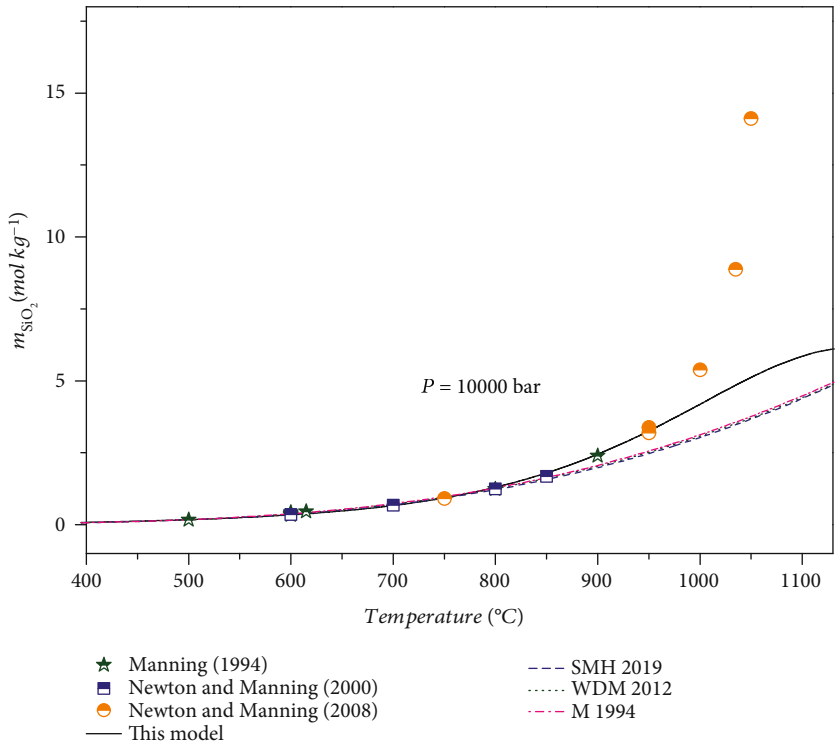


(a)

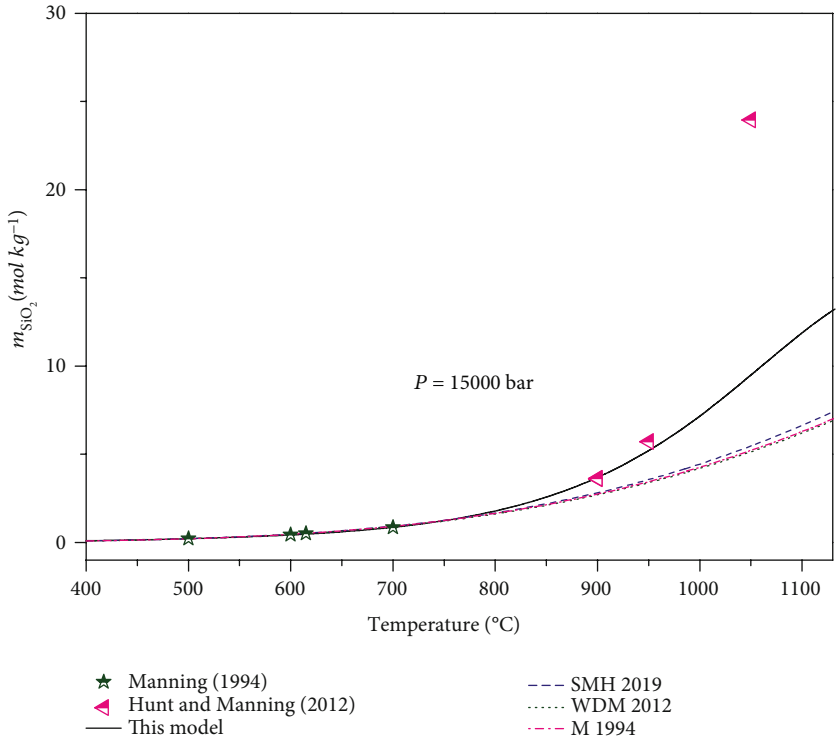


(b)

Figure 6: Continued.

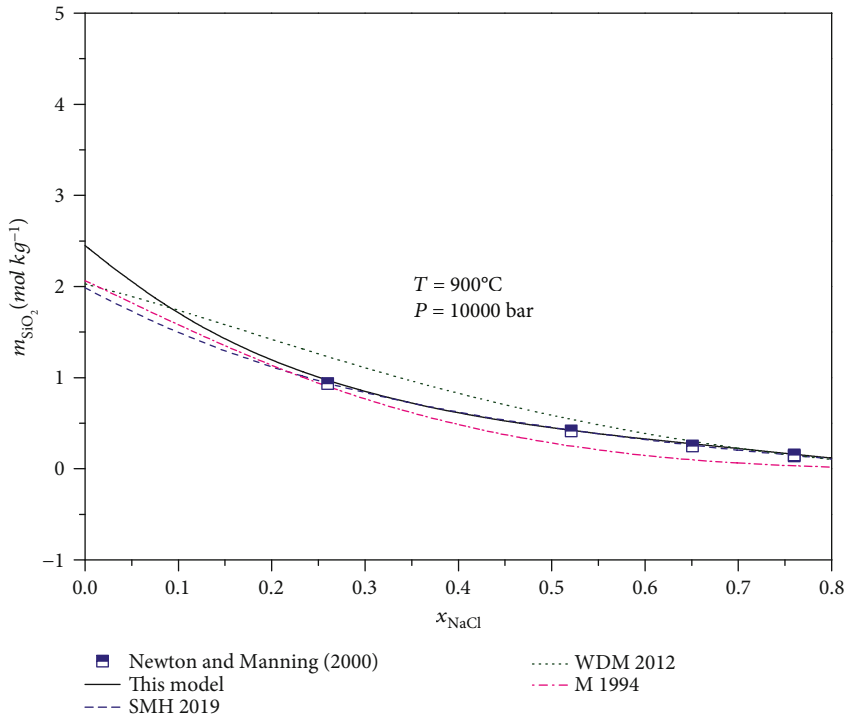


(c)

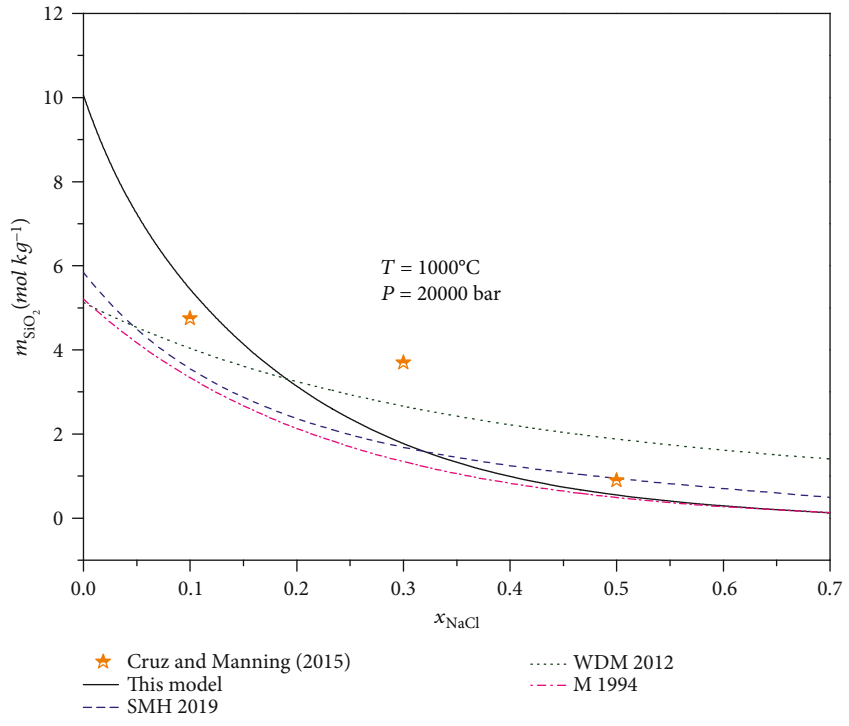


(d)

Figure 6: Comparisons of model extrapolation to high temperature and pressure hydrothermal conditions. (a, b) Computing results of different models in pure water. (c, d) Computing results of different models in $H_2O$-NaCl system. The solid curves, dash curves, dot curves, and dash dot curves present the predictions of this model, the SMH 2019 model, the WDM 2012 model, and the AD 2009 model, respectively.

points of Shmulovich et al. [21] in $H_2O$-$CO_2$ solutions as constant regression of their model as the initial zero of NaCl content. However, the experimental data of Shmulovich et al. [21] are systematically higher than the data of Shmulovich et al. [22] at the same $T$, $P$ and nearly the identical fluid composition conditions. Because of the higher experimental value

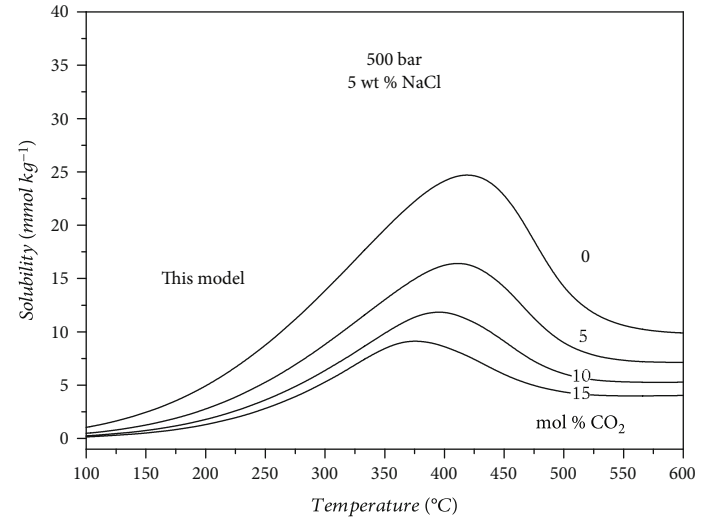


(a)

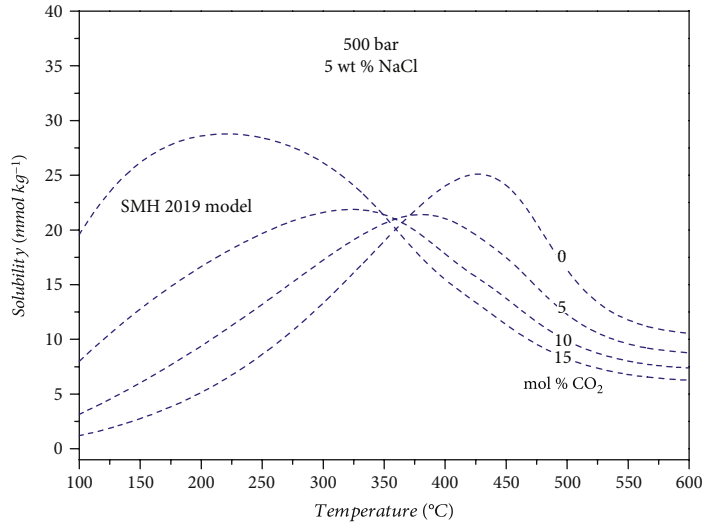


(b)

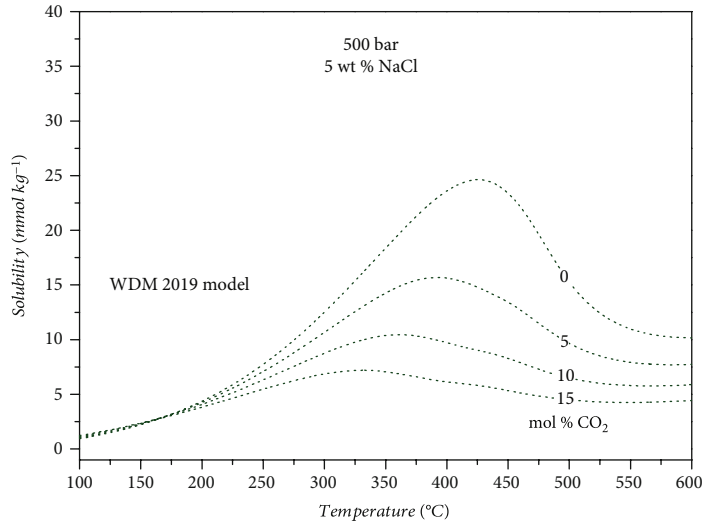


(c)

Figure 7: Continued.

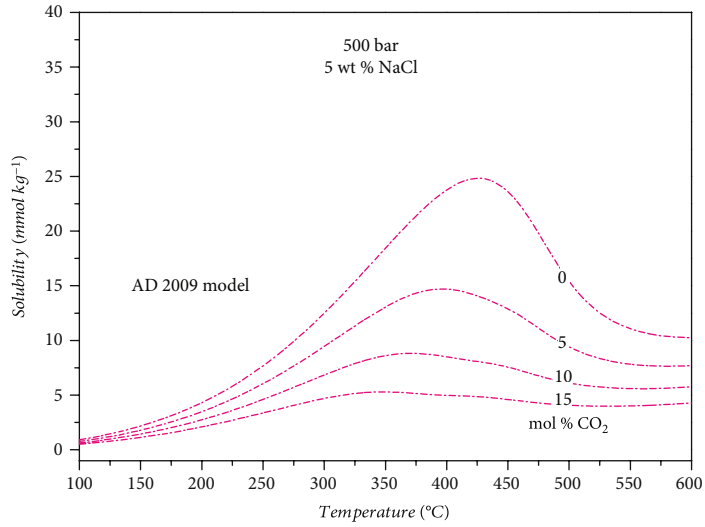


(d)

Figure 7: Comparisons of model predictions in $H_2O$-$CO_2$-NaCl hydrothermal fluids with fixed salinity and pressure conditions and with $CO_2$ compositions from 0 to 15 mol %.

SMH 2019 model adopted in constant regression, this may be the reason of their model's failure when used in $H_2O$-$CO_2$-NaCl fluid mixtures as Figure 7(b) denotes the paradox computing results (please note that when the temperature is below 350°C, the quartz solubility has enhanced follows the gradually adding of $CO_2$ with the same NaCl contents, whereas $CO_2$ as a nonelectrolyte which will always expand the fluid volume and consequently lower quartz solubility).

As we can see from the Figure 7, the simulating results have revealed that the four competitive quartz solubility models here discussed are all displayed "salting-in" effect at low pressure condition (500 bar). Except for the SMH 2019 model, the prediction ability of this model, the WDM 2012 model, and the AD model are all displayed monotonous lowering quartz solubility when gradually enhancing $CO_2$ content in the above ternary fluid systems at the same salinity conditions. In point of fact, we consider that the trends and overall ranges of this present model may probably correct and more accurate when used in the $H_2O$-$CO_2$-NaCl fluid mixtures (Figure 3(e) and 7(a)), whereas it still should be deeper tested by much more experimental data sets on quartz solubilities.

*4.3. Perspectives for Model Application.* A versatile understanding of solubility behaviors of silicate minerals (quartz in particular) in electrolyte and/or volatile-bearing aqueous fluids is vital in deciphering fundamental petrological and ore-forming processes in various geological settings [70]. For instance, in subduction zone, the chemical components in slab (subducting oceanic lithosphere) fluids (essentially metamorphic fluids [71]) may not only affect the chemical and isotopic signatures of arc-derived magmatic rocks [72], but also influence melting behavior of overriding mantle [73]. Similarly, solubility of mineral fluids in deep crust and upper mantle is critical in mass transport and evolution of the crust [20, 74]. Not surprisingly, solubility models applicable to these petrological settings with some extreme pressure and temperature conditions are prerequisite for a better understanding. The novel model of this study is among the best of such models.

In ore-forming environment, mostly encountered with middle to upper crust, solubility models with better precision and accuracy may significantly improve our understanding of fluid flow, fluid-rock interaction, and ore deposition [75]. A more accurate model may facilitate to distinguish subtle differences in solubility to fluid $P$ - $T$ - $x$ conditions (e.g., the model of Wei et al. [68]). For instance, it will enable the identification of retrograde solubility in complex $CO_2$-bearing aqueous fluids, which are very important for metal (e.g., Au and Cu) deposition (for porphyry deposit: [39, 40]; for orogenic Au deposit: [41, 68]). In addition, quartz solubility models may also be significant in studying many other settings, for instance, in migmatite [76] and pegmatite [77]. Therefore, there is no doubt that solubility model of this study, with its superior accuracy and wider application range, will provide an improved geochemical tool for geoscience community.

## 5. Conclusions

A density-based model on quartz solubility in pure water and NaCl and/or $CO_2$-bearing solutions has been developed in this work. This model is semiempirical and is based on the pervious results of the AD 2009 model and the WDM 2012 model. The success of this model is benefitted from two aspects: one is the logarithm linear relationship between quartz solubility and the density of pure water, and the other is the accurate thermodynamic model of Dubacq et al. [66] and Mao et al. [54] for water activity ($a_{H_2O}$) and molar volume of the fluid mixture ($V_{mix}$) calculating in $H_2O$-$CO_2$-NaCl systems. Compared to the experimental data sets and the existing most competitive models, the accuracy of this model has been greatly enhanced. Particularly, this model may be extrapolated to high temperature and pressure

conditions, provided new experimental data sets are available. It seems that the trends and overall ranges of this model may be probably correct and more accurate when used in the $H_2O$-$CO_2$-NaCl fluid mixtures. Moreover, this model can reproduce the retrograde and "salting-in" phenomenon on quartz solubility in pure water and NaCl-bearing solutions clearly and more accurate. At the same time, an algorithm on quartz solubility isopleths in the single-phase region based on this new model has first proposed.

## Data Availability

Detailed comparisons between the experimental data sets and the calculated results from different models on quartz solubility in pure water and $CO_2$ and/or NaCl-bearing solutions are summarized in supplementary A. Computing programs for quartz solubilities and them isopleths are embedded in two Fortran programs, and they can be obtained from Supplementary B or the website: https://www.researchgate.net/publication/345630311_Iso-solubility_quartz.

## Conflicts of Interest

The authors declare that they have no conflicts of interest.

## Acknowledgments

Two anonymous reviewers are acknowledged for their constructive comments. This research was jointly funded by the State Key Laboratory of Ore Deposit Geochemistry Foundation of Institute of Geochemistry, Chinese Academy of Sciences (No. 201707) and the National Natural Science Foundation of China (No. 41602073).

## Supplementary Materials

*Supplementary 1*. Supplementary A. Supplementary data. Detailed comparisons between the experimental data sets and the calculated results from different models on quartz solubility in pure water and $CO_2$ and/or NaCl-bearing solutions are summarized in the table (experimental data in italics are the ones not used in model parameterization procedure).

*Supplementary 2*. Supplementary B. Computing programs. Computing programs for quartz solubilities and them isopleths are embedded in two Fortran programs, and they can be obtained from below website: https://www.researchgate.net/publication/348834292_Supplementary_B.

## References

[1] J. Götze and R. Möckel, *Quartz: Deposits, Mineralogy and Analytics*, Springer Science & Business Media, 2012.

[2] R. O. Fournier, "A method of calculating quartz solubilities in aqueous sodium chloride solutions," *Geochimica et Cosmochimica Acta*, vol. 47, no. 3, pp. 579–586, 1983.

[3] R. O. Fournier, "Hydrothermal processes related to movement of fluid from plastic into brittle rock in the magmatic-epithermal environment," *Economic Geology*, vol. 94, no. 8, pp. 1193–1211, 1999.

[4] D. K. Weatherley and R. W. Henley, "Flash vaporization during earthquakes evidenced by gold deposits," *Nature Geoscience*, vol. 6, no. 4, pp. 294–298, 2013.

[5] B. Rusk and M. Reed, "Scanning electron microscope-cathodoluminescence analysis of quartz reveals complex growth histories in veins from the Butte porphyry copper deposit, Montana," *Geology*, vol. 30, no. 8, pp. 727–730, 2002.

[6] B. G. Rusk, H. A. Lowers, and M. H. Reed, "Trace elements in hydrothermal quartz: relationships to cathodoluminescent textures and insights into vein formation," *Geology*, vol. 36, no. 7, pp. 547–550, 2008.

[7] G. Lambrecht and L. W. Diamond, "Morphological ripening of fluid inclusions and coupled zone-refining in quartz crystals revealed by cathodoluminescence imaging: iImplications for CL-petrography, fluid inclusion analysis and trace-element geothermometry," *Geochimica et Cosmochimica Acta*, vol. 141, pp. 381–406, 2014.

[8] L. Maydagán, M. Franchini, B. Rusk et al., "Porphyry to epithermal transition in the altar Cu-(Au-Mo) deposit, Argentina, studied by cathodoluminescence, LA-ICP-MS, and fluid inclusion analysis," *Economic Geology*, vol. 110, no. 4, pp. 889–923, 2015.

[9] G. C. Kennedy, "A portion of the system silica-water," *Economic Geology*, vol. 45, no. 7, pp. 629–653, 1950.

[10] G. W. Morey and J. M. Hesselgesser, "The solubility of quartz and some other substances in superheated steam at high pressures," *Transactions of the American Society of Mechanical Engineers*, vol. 73, pp. 864–875, 1951.

[11] S. Kitahara, "The solubility of quartz in water at high temperatures and high pressures," *Review of Physical Chemistry of Japan*, vol. 30, pp. 109–114, 1960.

[12] J. A. Van Lier, P. L. De Bruyn, and J. T. G. Overbeek, "The solubility of quartz," *The Journal of Physical Chemistry*, vol. 64, no. 11, pp. 1675–1682, 1960.

[13] G. W. Morey, R. O. Fournier, and J. J. Rowe, "The solubility of quartz in water in the temperature interval from 25 °C to 300 °C," *Geochimica et Cosmochimica Acta*, vol. 26, no. 10, pp. 1029–1043, 1962.

[14] R. Siever, "Silica solubility, 0-200 °C, and the diagenesis of siliceous sediments," *Journal of Geology*, vol. 70, no. 2, pp. 127–150, 1962.

[15] D. F. Weill and W. S. Fyfe, "The solubility of quartz in $H_2O$ in the range 1000-4000 bars and 400-550 °C," *Geochimica et Cosmochimica Acta*, vol. 28, no. 8, pp. 1243–1255, 1964.

[16] G. M. Anderson and C. W. Burnham, "The solubility of quartz in supercritical water," *American Journal of Science*, vol. 263, no. 6, pp. 494–511, 1965.

[17] G. M. Anderson and C. W. Burnham, "Reactions of quartz and corundum with aqueous chloride and hydroxide solutions at high temperatures and pressures," *American Journal of Science*, vol. 265, no. 1, pp. 12–27, 1967.

[18] D. A. Crerar and G. M. Anderson, "Solubility and solutions reactions of quartz in dilute hydrothermal solutions," *Chemical Geology*, vol. 8, no. 2, pp. 107–122, 1971.

[19] J. V. Walther and H. C. Helgeson, "Calculation of the thermodynamic properties of aqueous silica and the solubility of quartz and its polymorphs at high pressures and temperatures," *American Journal of Science*, vol. 277, no. 10, pp. 1315–1351, 1977.

[20] R. C. Newton and C. E. Manning, "Quartz solubility in $H_2O$-NaCl and $H_2O$-$CO_2$ solutions at deep crust-upper mantle pressures and temperatures: 2-15 kbar and 500-900 °C," *Geochimica et Cosmochimica Acta*, vol. 64, no. 17, pp. 2993–3005, 2000.

[21] K. I. Shmulovich, C. M. Graham, and B. W. D. Yardley, "Quartz, albite and diopside solubilities in $H_2O$-NaCl and $H_2O$-$CO_2$ fluids at 0.5-0.9 GPa," *Contributions to Mineralogy and Petrology*, vol. 141, no. 1, pp. 95–108, 2001.

[22] K. I. Shmulovich, B. W. D. Yardley, and C. M. Graham, "The solubility of quartz in crustal fluids: experiments and general equations for salt solutions and $H_2O$-$CO_2$ mixtures at 400-800 °C and 0.1-0.9 GPa," *Geofluids*, vol. 6, no. 2, pp. 154–167, 2006.

[23] J. D. Hunt and C. E. Manning, "A thermodynamic model for the system $SiO_2$-$H_2O$ near the upper critical end point based on quartz solubility experimentsat 500-1100 °C and 5-20 kbar," *Geochimica et Cosmochimica Acta*, vol. 86, pp. 196–213, 2012.

[24] M. F. Cruz and C. E. Manning, "Experimental determination of quartz solubility and melting in the system $SiO_2$-$H_2O$-NaCl at 15-20 kbar and 900-1100 °C: implications for silica polymerization and the formation of supercritical fluids," *Contributions to Mineralogy and Petrology*, vol. 170, no. 4, p. 35, 2015.

[25] I. G. Ganeyev, "Solubility and crystallization of silica in chloride," *Doklady Academii Nauk SSSR*, vol. 224, pp. 248–250, 1975.

[26] P. G. Novgorodov, "On the solubility of quartz in $H_2O$+$CO_2$ and $H_2O$+NaCl at 700 °C and 1.5 kb pressure," *Geochemistry International*, vol. 14, no. 4, pp. 191–193, 1977.

[27] R. O. Fournier, R. J. Rosenbauer, and J. L. Bischoff, "The solubility of quartz in aqueous sodium chloride solution at 350 °C and 180 to 500 bars," *Geochimica et Cosmochimica Acta*, vol. 46, no. 10, pp. 1975–1978, 1982.

[28] Z. X. Xie and J. V. Walther, "Quartz solubilities in NaCl solutions with and without wollastonite at elevated temperatures and pressures," *Geochimica et Cosmochimica Acta*, vol. 57, no. 9, pp. 1947–1955, 1993.

[29] J. V. Walther and P. M. Orville, "The extraction-quench technique for determination of the thermodynamic properties of solute complexes: application to quartz solubility in fluid mixtures," *American Mineralogist*, vol. 68, pp. 731–741, 1983.

[30] C. E. Manning, "The solubility of quartz in the lower crust and upper mantle," *Geochimica et Cosmochimica Acta*, vol. 58, no. 22, pp. 4831–4839, 1994.

[31] R. C. Newton and C. E. Manning, "Thermodynamics of $SiO_2$ - $H_2O$ fluid near the upper critical end point from quartz solubility measurements at 10kbar," *Earth and Planetary Science Letters*, vol. 274, no. 1-2, pp. 241–249, 2008.

[32] C. E. Manning, A. Antignano, and H. A. Lin, "Premelting polymerization of crustal and mantle fluids, as indicated by the solubility of albite+paragonite+quartz in $H_2O$ at 1 GPa and 350~620 °C," *Earth and Planetary Science Letters*, vol. 292, no. 3-4, pp. 325–336, 2010.

[33] H. C. Helgeson, D. H. Kirkham, and G. C. Flowers, "Theoretical prediction of the thermodynamic behavior of aqueous electrolytes at high pressures and temperatures. IV. Calculation of activity coefficients, osmotic coefficients and apparent molal and standard and relative molal properties to 600 °C and 5 kb," *American Journal of Science*, vol. 281, no. 10, pp. 1249–1516, 1981.

[34] E. L. Shock, H. C. Helgeson, and D. A. Sverjensky, "Calculation of the thermodynamic and transport properties of aqueous species at high pressures and temperatures: standard partial molal properties of inorganic neutral species," *Geochimica et Cosmochimica Acta*, vol. 53, no. 9, pp. 2157–2183, 1989.

[35] N. N. Akinfiev and L. W. Diamond, "A simple predictive model of quartz solubility in water-salt-$CO_2$ systems at temperatures up to 1000 °C and pressures up to 1000MPa," *Geochimica et Cosmochimica Acta*, vol. 73, no. 6, pp. 1597–1608, 2009.

[36] Q. Wei, Z. H. Duan, and S. D. Mao, "A thermodynamic model of quartz solubility in $H_2O$-$CO_2$-NaCl systems up to 1000 °C and 1.5 GP," *Acta Petrologica Sinica*, vol. 28, no. 8, pp. 2656–2666, 2012.

[37] X. Shi, S. Mao, J. Hu, J. Zhang, and J. Zheng, "An accurate model for the solubilities of quartz in aqueous NaCl and/or $CO_2$ solutions at temperatures up to 1273 K and pressures up to 20,000 bar," *Chemical Geology*, vol. 513, pp. 73–87, 2019.

[38] H. L. Brooks and M. Steele-MacInnis, "A model for the solubility of minerals in saline aqueous fluids in the crust and upper mantle," *American Journal of Science*, vol. 319, no. 9, pp. 754–787, 2019.

[39] T. Monecke, J. Monecke, T. J. Reynolds et al., "Quartz solubility in the $H_2O$-NaCl system: a framework for understanding vein formation in porphyry copper deposits," *Economic Geology*, vol. 113, no. 5, pp. 1007–1046, 2018.

[40] T. Monecke, J. Monecke, and T. J. Reynolds, "The influence of $CO_2$ on the solubility of quartz in single-phase hydrothermal fluids: implications for the formation of stockwork veins in porphyry copper deposits," *Economic Geology*, vol. 114, no. 6, pp. 1195–1206, 2019.

[41] X. H. Li, Y. I. Klyukin, M. Steele-MacInnis, H. R. Fan, K. F. Yang, and B. Zoheir, "Phase equilibria, thermodynamic properties, and solubility of quartz in saline-aqueous-carbonic fluids: aApplication to orogenic and intrusion-related gold deposits," *Geochimica et Cosmochimica Acta*, vol. 283, pp. 201–221, 2020.

[42] R. Mosebach, "Thermodynamic behavior of quartz and other forms of silica in pure water at elevated temperatures and pressures with conclusions on their mechanism of solution," *Journal of Geology*, vol. 65, no. 4, pp. 347–363, 1957.

[43] R. O. Fournier and R. W. Potter II, "An equation correlating the solubility of quartz in water from 25 °C to 900 °C at pressures up to 10,000 bars," *Geochimica et Cosmochimica Acta*, vol. 46, no. 10, pp. 1969–1973, 1982.

[44] K. L. Von Damm, J. L. Bischoff, and R. J. Rosenbauer, "Quartz solubility in hydrothermal seawater: an experimental study and equation describing quartz solubility for up to 0.5m NaCl solutions," *American Journal of Science*, vol. 291, no. 10, pp. 977–1007, 1991.

[45] W. Wagner and A. Pruß, "The IAPWS formulation 1995 for the thermodynamic properties of ordinary water substance for general and scientific use," *Journal of Physical and Chemical Reference Data*, vol. 31, no. 2, pp. 387–535, 2002.

[46] E. U. Franck, "Hochverdichteter Wassedampf II. Ionendissociation von KCl in $H_2O$ bis 750 °C," *Zeitschrift für Physikalische Chemie*, vol. 8, no. 1_2, pp. 107–126, 1956.

[47] A. S. Quist, "The ionization constant of water to 800 °C and 4000 bars," *The Journal of Physical Chemistry*, vol. 74, pp. 3393–3402, 1970.

[48] W. L. Marshall, "A further description of complete equilibrium constants," *The Journal of Physical Chemistry*, vol. 76, no. 5, pp. 720–731, 1972.

[49] R. E. Mesmer, W. L. Marshall, D. A. Palmer, J. M. Simonson, and H. F. Holmes, "Thermodynamics of aqueous association and ionization reactions at high temperatures and pressures," *Journal of Solution Chemistry*, vol. 17, no. 8, pp. 699–718, 1988.

[50] W. L. Marshall and E. U. Franck, "Ion product of water substance, 0-1000 °C, 1-10,000 bars, new international formulation and its background," *Journal of Physical and Chemical Reference Data*, vol. 10, no. 2, pp. 295–304, 1981.

[51] J. J. Hemley, J. W. Montoya, J. W. Marinenko, and R. W. Luce, "Equilibria in the system $Al_2O_3$-$SiO_2$-$H_2O$ and some general implications for alteration-NOT/mineralization processes," *Economic Geology*, vol. 75, no. 2, pp. 210–228, 1980.

[52] R. H. Stokes and R. A. Robinson, "Ionic hydration and activity in electrolyte solutions," *Journal of the American Chemical Society*, vol. 70, no. 5, pp. 1870–1878, 1948.

[53] N. Zotov and H. Keppler, "Silica speciation in aqueous fluids at high pressures and temperatures," *Chemical Geology*, vol. 184, no. 1-2, pp. 71–82, 2002.

[54] S. D. Mao, Z. H. Duan, J. W. Hu, and D. H. Zhang, "A model for single phase PVTx properties of $CO_2$-$CH_4$-$C_2H_6$-$N_2$-$H_2O$-NaCl fluid mixtures from 273 to 1273 K and from 1 to 5000 bar," *Chemical Geology*, vol. 275, no. 3-4, pp. 148–160, 2010.

[55] C. J. van Nieuwenburg and M. P. M. van Zon, "Semi-quantitative measurements of the solubility of quartz in super-critical steam," *Recueil des Travaux Chimiques des Pays-Bas*, vol. 54, no. 2, pp. 129–132, 1935.

[56] R. O. Fournier, "Solubility of quartz in water in the temperature interval from 25 °C to 300 °C," *Geological Society of America Bulletin*, vol. 71, pp. 1867-1868, 1960.

[57] G. M. Anderson and C. W. Burnham, "Feldspar solubility and the transport of aluminum under metamorphic conditions," *American Journal of Science*, vol. 283-A, pp. 283–297, 1983.

[58] K. Vala Ragnarsdóttir and J. V. Walther, "Pressure sensitive "silica geothermometer" determined from quartz solubility experiments at 250 °C," *Geochimica et Cosmochimica Acta*, vol. 47, no. 5, pp. 941–946, 1983.

[59] D. G. Archer, "Thermodynamic properties of the NaCl+$H_2O$ system II. Thermodynamic properties of $NaCl_{(aq)}$, NaCl·2-$H_2O_{(cr)}$, and phase equilibria," *Journal of Physical and Chemical Reference Data*, vol. 21, no. 4, pp. 793–829, 1992.

[60] J. D. Rimstidt, "Quartz solubility at low temperatures," *Geochimica et Cosmochimica Acta*, vol. 61, no. 13, pp. 2553–2558, 1997.

[61] H. M. Wang, G. S. Henderson, and J. M. Brenan, "Measuring quartz solubility by in situ weight-loss determination using a hydrothermal diamond cell," *Geochimica et Cosmochimica Acta*, vol. 68, no. 24, pp. 5197–5204, 2004.

[62] R. C. Newton and C. E. Manning, "Hydration state and activity of aqueous silica in $H_2O$-$CO_2$ fluids at high pressure and temperature," *American Mineralogist*, vol. 94, no. 8-9, pp. 1287–1290, 2009.

[63] R. C. Newton and C. E. Manning, "Solubilities of corundum, wollastonite and quartz in $H_2O$-NaCl solutions at 800 °C and 10kbar: iInteraction of simple minerals with brines at high pressure and temperature," *Geochimica et Cosmochimica Acta*, vol. 70, no. 22, pp. 5571–5582, 2006.

[64] D. I. Foustoukos and W. E. Seyfried Jr., "Quartz solubility in the two-phase and critical region of the NaCl-KCl-$H_2O$ system: implications for submarine hydrothermal vent systems at 9°50' N East Pacific Rise," *Geochimica et Cosmochimica Acta*, vol. 71, no. 1, pp. 186–201, 2007.

[65] P. P. Scheuermann, C. Tan, and W. E. Seyfried, "Quartz solubility in the two-phase region of the NaCl-$H_2O$ system: an experimental study with application to the Piccard hydrothermal field, mid-Cayman rise," *Geochemistry, Geophysics, Geosystems*, vol. 19, no. 9, pp. 3570–3582, 2018.

[66] B. Dubacq, M. J. Bickle, and K. A. Evans, "An activity model for phase equilibria in the $H_2O$-$CO_2$-NaCl system," *Geochimica et Cosmochimica Acta*, vol. 110, pp. 229–252, 2013.

[67] M. Steele-MacInnis, L. Han, R. P. Lowell, J. D. Rimstidt, and R. J. Bodnar, "Quartz precipitation and fluid inclusion characteristics in sub-seafloor hydrothermal systems associated with volcanogenic massive sulfide deposits," *Central European Journal of Geosciences*, vol. 4, pp. 275–286, 2012.

[68] Q. Wei, H. R. Fan, J. Pironon, and X. Liu, "Auriferous quartz veining due to $CO_2$ content variations and decompressional cooling, revealed by quartz solubility, SEM-CL and fluid inclusion analyses (The Linglong Goldfield, Jiaodong)," *Minerals*, vol. 10, no. 5, p. 417, 2020.

[69] S. D. Mao, D. H. Zhang, Y. Q. Li, and N. Q. Liu, "An improved model for calculating $CO_2$ solubility in aqueous NaCl solutions and application to $CO_2$-$H_2O$-NaCl fluid inclusions," *Chemical Geology*, vol. 347, pp. 43–58, 2013.

[70] D. Dolejš and C. E. Manning, "Thermodynamic model for mineral solubility in aqueous fluids: theory, calibration and application to model fluid-flow systems," *Geofluids*, vol. 10, 40 pages, 2010.

[71] W. Heinrich, "Fluid immiscibility in metamorphic rocks," *Reviews in Mineralogy & Geochemistry*, vol. 12, no. 65, pp. 389–430, 2007.

[72] M. Scambelluri and P. Philippot, "Deep fluids in subduction zones," *Lithos*, vol. 55, no. 1-4, pp. 213–227, 2001.

[73] J. E. Mungall, "Roasting the mantle: slab melting and the genesis of major Au and Au-rich Cu deposits," *Geological Society of America*, vol. 30, no. 10, pp. 915–918, 2002.

[74] J. J. Ague, *Fluid Flow in the Deep Crust*, Yale University, New Haven, CT, USA, 2014.

[75] C. A. Heinrich and P. A. Candela, *Fluids and Ore Formation in the earth's Crust*, University of Zurich, Zurich, Switzerland, University of Maryland, College Park, MD, USA, 2014.

[76] L. S. Hollister, "On the origin of $CO_2$-rich fluid inclusions in migmatites," *Journal of Metamorphic Geology*, vol. 6, no. 4, pp. 467–474, 1988.

[77] R. Thomas, J. D. Webster, and P. Davidson, "Understanding pegmatite formation: the melt and fluid inclusion approach," *Mineralogical Association of Canada Short Course*, vol. 36, pp. 189–210, 2006.